

Higgs Boson Masses and Couplings in the Minimal Supersymmetric Model

Howard E. Haber

*Santa Cruz Institute for Particle Physics
University of California, Santa Cruz, CA 95064, U.S.A.*

Abstract

The Higgs sector of the Minimal Supersymmetric Model (MSSM) is a CP-conserving two-Higgs doublet model that depends, at tree-level, on two Higgs sector parameters. In order to accurately determine the phenomenological implications of this model, one must include the effects of radiative corrections. The leading contributions to the one-loop radiative corrections are exhibited; large logarithms are resummed by the renormalization group method. Implications for Higgs phenomenology are briefly discussed.

To appear in *Perspectives on Higgs Physics II*
Gordon L. Kane, editor (World Scientific, Singapore, 1997)

Higgs Boson Masses and Couplings in the Minimal Supersymmetric Model

Howard E. Haber

*Santa Cruz Institute for Particle Physics
University of California, Santa Cruz, CA 95064*

Abstract

The Higgs sector of the Minimal Supersymmetric Model (MSSM) is a CP-conserving two-Higgs doublet model that depends, at tree-level, on two Higgs sector parameters. In order to accurately determine the phenomenological implications of this model, one must include the effects of radiative corrections. The leading contributions to the one-loop radiative corrections are exhibited; large logarithms are resummed by the renormalization group method. Implications for Higgs phenomenology are briefly discussed.

1 Introduction

The Standard Model with minimal Higgs content is not expected to be the ultimate theoretical structure responsible for electroweak symmetry breaking [1,2]. If the Standard Model is embedded in a more fundamental structure characterized by a much larger energy scale (*e.g.*, the Planck scale, which must appear in any theory of fundamental particles and interactions that includes gravity), the Higgs boson would tend to acquire mass of order the largest energy scale due to radiative corrections. Only by adjusting (*i.e.*, “fine-tuning”) the parameters of the Higgs potential “unnaturally” can one arrange a large hierarchy between the Planck scale and the scale of electroweak symmetry breaking [3,4]. The Standard Model provides no mechanism for this, but supersymmetric theories have the potential to address these issues. In a supersymmetric theory, the size of radiative corrections to scalar squared-masses is limited by the exact cancelation of quadratically divergent contributions from loops of particles and their supersymmetric partners. Since supersymmetry is not an exact symmetry at low energies, this cancelation must be incomplete, and the size of the radiative corrections to the Higgs mass is controlled by the extent of the supersymmetry breaking. The resolution of the naturalness and hierarchy problems requires that the scale of supersymmetry breaking should

not exceed $\mathcal{O}(1 \text{ TeV})$ [5]. Such “low-energy” supersymmetric theories are especially interesting in that, to date, they provide the only theoretical framework in which the problems of naturalness and hierarchy can be resolved while retaining the Higgs bosons as truly elementary weakly coupled spin-0 particles.

The Minimal Supersymmetric extension of the Standard Model (MSSM) contains the Standard Model particle spectrum and the corresponding supersymmetric partners [6,7]. In addition, the MSSM must possess two Higgs doublets in order to give masses to up and down type fermions in a manner consistent with supersymmetry (and to avoid gauge anomalies introduced by the fermionic superpartners of the Higgs bosons). In particular, the MSSM Higgs sector is a CP-conserving two-Higgs-doublet model, which can be parametrized at tree-level in terms of two Higgs sector parameters. This structure arises due to constraints imposed by supersymmetry that determine the Higgs quartic couplings in terms of electroweak gauge coupling constants.

In section 2, I review the general structure of the (nonsupersymmetric) two-Higgs-doublet extension of the Standard Model. By imposing the constraints of supersymmetry on the quartic terms of the Higgs potential (and the Higgs-fermion interaction) one obtains the Higgs sector of the MSSM. The tree-level predictions of this model are briefly summarized in section 3. The inclusion of radiative corrections in the analysis of the MSSM Higgs sector can have profound implications. The most dramatic effect of the radiative corrections on the MSSM Higgs sector is the modification of the tree-level mass relations of the model. The leading one-loop radiative corrections to MSSM Higgs masses are described in section 4. These include the full set of one-loop leading logarithmic terms, and the leading third generation squark-mixing corrections. In section 5, the leading logarithms are resummed to all orders via the renormalization group technique. A simple analytic formula is exhibited which serves as an excellent approximation to the numerically integrated renormalization group equations. Numerical examples demonstrate that the Higgs masses computed in this approximation lie within 2 GeV of their actual values over a very large fraction of the supersymmetric parameter space. Finally, some implications of the radiatively-corrected Higgs sector are briefly explored in section 6. Certain technical details are relegated to the appendices.

2 The Two-Higgs Doublet Model

I begin with a brief review of the general (non-supersymmetric) two-Higgs doublet extension of the Standard Model [8]. Let Φ_1 and Φ_2 denote two complex $Y = 1$, $SU(2)_L$ doublet scalar fields. The most general gauge invariant scalar potential is given by

$$\begin{aligned}
\mathcal{V} = & m_{11}^2 \Phi_1^\dagger \Phi_1 + m_{22}^2 \Phi_2^\dagger \Phi_2 - [m_{12}^2 \Phi_1^\dagger \Phi_2 + \text{h.c.}] \\
& + \frac{1}{2} \lambda_1 (\Phi_1^\dagger \Phi_1)^2 + \frac{1}{2} \lambda_2 (\Phi_2^\dagger \Phi_2)^2 + \lambda_3 (\Phi_1^\dagger \Phi_1) (\Phi_2^\dagger \Phi_2) + \lambda_4 (\Phi_1^\dagger \Phi_2) (\Phi_2^\dagger \Phi_1) \\
& + \left\{ \frac{1}{2} \lambda_5 (\Phi_1^\dagger \Phi_2)^2 + [\lambda_6 (\Phi_1^\dagger \Phi_1) + \lambda_7 (\Phi_2^\dagger \Phi_2)] \Phi_1^\dagger \Phi_2 + \text{h.c.} \right\}. \tag{1}
\end{aligned}$$

In most discussions of two-Higgs-doublet models, the terms proportional to λ_6 and λ_7 are absent. This can be achieved by imposing a discrete symmetry $\Phi_1 \rightarrow -\Phi_1$ on the model. Such a symmetry would also require $m_{12} = 0$ unless we allow a soft violation of this discrete symmetry by dimension-two terms.¹ For the moment, I will refrain from setting any of the coefficients in eq. (1) to zero. In principle, m_{12}^2 , λ_5 , λ_6 and λ_7 can be complex. However, for simplicity, I shall ignore the possibility of CP-violating effects in the Higgs sector by choosing all coefficients in eq. (1) to be real. The scalar fields will develop non-zero vacuum expectation values if the mass matrix m_{ij}^2 has at least one negative eigenvalue. Imposing CP invariance and $U(1)_{\text{EM}}$ gauge symmetry, the minimum of the potential is

$$\langle \Phi_1 \rangle = \frac{1}{\sqrt{2}} \begin{pmatrix} 0 \\ v_1 \end{pmatrix}, \quad \langle \Phi_2 \rangle = \frac{1}{\sqrt{2}} \begin{pmatrix} 0 \\ v_2 \end{pmatrix}, \tag{2}$$

where the v_i are assumed to be real. It is convenient to introduce the following notation:

$$v^2 \equiv v_1^2 + v_2^2 = \frac{4m_W^2}{g^2} = (246 \text{ GeV})^2, \quad t_\beta \equiv \tan \beta \equiv \frac{v_2}{v_1}. \tag{3}$$

Of the original eight scalar degrees of freedom, three Goldstone bosons (G^\pm and G^0) are absorbed (“eaten”) by the W^\pm and Z . The remaining five physical Higgs particles are: two CP-even scalars (h^0 and H^0 , with $m_{h^0} \leq m_{H^0}$), one CP-odd scalar (A^0) and a charged Higgs pair (H^\pm). The mass parameters m_{11} and m_{22} can be eliminated by minimizing the scalar potential. The resulting squared masses for the CP-odd and charged Higgs states are

$$\begin{aligned}
m_{A^0}^2 &= \frac{m_{12}^2}{s_\beta c_\beta} - \frac{1}{2} v^2 (2\lambda_5 + \lambda_6 t_\beta^{-1} + \lambda_7 t_\beta), \\
m_{H^\pm}^2 &= m_{A^0}^2 + \frac{1}{2} v^2 (\lambda_5 - \lambda_4). \tag{4}
\end{aligned}$$

¹This latter requirement is sufficient to guarantee the absence of Higgs-mediated tree-level flavor changing neutral currents.

The two CP-even Higgs states mix according to the following squared mass matrix:

$$\mathcal{M}^2 = m_{A^0}^2 \begin{pmatrix} s_\beta^2 & -s_\beta c_\beta \\ -s_\beta c_\beta & c_\beta^2 \end{pmatrix} + v^2 \begin{pmatrix} \lambda_1 c_\beta^2 + 2\lambda_6 s_\beta c_\beta + \lambda_5 s_\beta^2 & (\lambda_3 + \lambda_4)s_\beta c_\beta + \lambda_6 c_\beta^2 + \lambda_7 s_\beta^2 \\ (\lambda_3 + \lambda_4)s_\beta c_\beta + \lambda_6 c_\beta^2 + \lambda_7 s_\beta^2 & \lambda_2 s_\beta^2 + 2\lambda_7 s_\beta c_\beta + \lambda_5 c_\beta^2 \end{pmatrix}, \quad (5)$$

where $s_\beta \equiv \sin \beta$ and $c_\beta \equiv \cos \beta$. The physical mass eigenstates are

$$\begin{aligned} H^0 &= (\sqrt{2}\text{Re } \Phi_1^0 - v_1) \cos \alpha + (\sqrt{2}\text{Re } \Phi_2^0 - v_2) \sin \alpha, \\ h^0 &= -(\sqrt{2}\text{Re } \Phi_1^0 - v_1) \sin \alpha + (\sqrt{2}\text{Re } \Phi_2^0 - v_2) \cos \alpha. \end{aligned} \quad (6)$$

The corresponding masses are

$$m_{H^0, h^0}^2 = \frac{1}{2} \left[\mathcal{M}_{11}^2 + \mathcal{M}_{22}^2 \pm \sqrt{(\mathcal{M}_{11}^2 - \mathcal{M}_{22}^2)^2 + 4(\mathcal{M}_{12}^2)^2} \right], \quad (7)$$

and the mixing angle α is obtained from

$$\begin{aligned} \sin 2\alpha &= \frac{2\mathcal{M}_{12}^2}{\sqrt{(\mathcal{M}_{11}^2 - \mathcal{M}_{22}^2)^2 + 4(\mathcal{M}_{12}^2)^2}}, \\ \cos 2\alpha &= \frac{\mathcal{M}_{11}^2 - \mathcal{M}_{22}^2}{\sqrt{(\mathcal{M}_{11}^2 - \mathcal{M}_{22}^2)^2 + 4(\mathcal{M}_{12}^2)^2}}. \end{aligned} \quad (8)$$

The phenomenology of the two-Higgs doublet model depends in detail on the various couplings of the Higgs bosons to gauge bosons, Higgs bosons and fermions. The Higgs couplings to gauge bosons follow from gauge invariance and are thus model independent. For example, the couplings of the two CP-even Higgs bosons to W and Z pairs are given in terms of the angles α and β by

$$\begin{aligned} g_{h^0 VV} &= g_V m_V \sin(\beta - \alpha) \\ g_{H^0 VV} &= g_V m_V \cos(\beta - \alpha), \end{aligned} \quad (9)$$

where

$$g_V \equiv \begin{cases} g, & V = W, \\ g/\cos \theta_W, & V = Z. \end{cases} \quad (10)$$

There are no tree-level couplings of A^0 or H^\pm to VV . Gauge invariance also determines the strength of the trilinear couplings of one gauge boson to two Higgs bosons. For example,

$$\begin{aligned} g_{h^0 A^0 Z} &= \frac{g \cos(\beta - \alpha)}{2 \cos \theta_W}, \\ g_{H^0 A^0 Z} &= \frac{-g \sin(\beta - \alpha)}{2 \cos \theta_W}. \end{aligned} \quad (11)$$

In the examples shown above, some of the couplings can be suppressed if either $\sin(\beta - \alpha)$ or $\cos(\beta - \alpha)$ is very small. Note that all the vector boson–Higgs boson couplings cannot vanish simultaneously. From the expressions above, we see that the following sum rules must hold separately for $V = W$ and Z :

$$\begin{aligned} g_{H^0 V V}^2 + g_{h^0 V V}^2 &= g_V^2 m_V^2, \\ g_{h^0 A^0 Z}^2 + g_{H^0 A^0 Z}^2 &= \frac{g^2}{4 \cos^2 \theta_W}. \end{aligned} \quad (12)$$

These results are a consequence of the tree-unitarity of the electroweak theory [9]. Moreover, if we focus on a given CP-even Higgs state, we note that its couplings to VV and $A^0 V$ cannot be simultaneously suppressed, since eqs. (9)–(11) imply that

$$g_{h Z Z}^2 + 4 m_Z^2 g_{h A^0 Z}^2 = \frac{g^2 m_Z^2}{\cos^2 \theta_W}, \quad (13)$$

for $h = h^0$ or H^0 . Similar considerations also hold for the coupling of h^0 and H^0 to $W^\pm H^\mp$. We can summarize the above results by noting that the coupling of h^0 and H^0 to vector boson pairs or vector–scalar boson final states is proportional to either $\sin(\beta - \alpha)$ or $\cos(\beta - \alpha)$ as indicated below [1,10].

$$\begin{array}{ll} \frac{\cos(\beta - \alpha)}{H^0 W^+ W^-} & \frac{\sin(\beta - \alpha)}{h^0 W^+ W^-} \\ \frac{H^0 Z Z}{Z A^0 h^0} & \frac{h^0 Z Z}{Z A^0 H^0} \\ \frac{W^\pm H^\mp h^0}{Z W^\pm H^\mp h^0} & \frac{W^\pm H^\mp H^0}{Z W^\pm H^\mp H^0} \\ \frac{\gamma W^\pm H^\mp h^0}{\gamma W^\pm H^\mp H^0} & \frac{\gamma W^\pm H^\mp H^0}{\gamma W^\pm H^\mp H^0} \end{array} \quad (14)$$

Note in particular that *all* vertices in the theory that contain at least one vector boson and *exactly one* non-minimal Higgs boson state (H^0 , A^0 or H^\pm) are proportional to $\cos(\beta - \alpha)$.

The 3-point and 4-point Higgs self-couplings depend on the parameters of the two-Higgs-doublet potential [eq. (1)]. The Feynman rules for the trilinear Higgs vertices are listed in Appendix A. The Feynman rules for the 4-point Higgs vertices are rather tedious in the general two-Higgs-doublet model and will not be given here.

The Higgs couplings to fermions are model dependent, although their form is often constrained by discrete symmetries that are imposed in order to avoid tree-level flavor changing neutral currents mediated by Higgs exchange [11]. An example of a model that respects this constraint is one in which one Higgs doublet (before symmetry breaking) couples exclusively to down-type fermions and the other Higgs

doublet couples exclusively to up-type fermions. This is the pattern of couplings found in the MSSM. The results in this case are as follows. The couplings of the neutral Higgs bosons to $f\bar{f}$ relative to the Standard Model value, $gm_f/2m_W$, are given by (using 3rd family notation)

$$\begin{aligned}
h^0 b\bar{b} : \quad & -\frac{\sin \alpha}{\cos \beta} = \sin(\beta - \alpha) - \tan \beta \cos(\beta - \alpha), \\
h^0 t\bar{t} : \quad & \frac{\cos \alpha}{\sin \beta} = \sin(\beta - \alpha) + \cot \beta \cos(\beta - \alpha), \\
H^0 b\bar{b} : \quad & \frac{\cos \alpha}{\cos \beta} = \cos(\beta - \alpha) + \tan \beta \sin(\beta - \alpha), \\
H^0 t\bar{t} : \quad & \frac{\sin \alpha}{\sin \beta} = \cos(\beta - \alpha) - \cot \beta \sin(\beta - \alpha), \\
A^0 b\bar{b} : \quad & \gamma_5 \tan \beta, \\
A^0 t\bar{t} : \quad & \gamma_5 \cot \beta,
\end{aligned} \tag{15}$$

(the γ_5 indicates a pseudoscalar coupling), and the charged Higgs boson coupling to fermion pairs (with all particles pointing into the vertex) is given by

$$g_{H^\pm t\bar{b}} = \frac{g}{2\sqrt{2}m_W} [m_t \cot \beta (1 + \gamma_5) + m_b \tan \beta (1 - \gamma_5)]. \tag{16}$$

The pattern of couplings displayed above can be understood in the context of the *decoupling limit* of the two-Higgs-doublet model [12,13]. First, consider the Standard Model Higgs boson (ϕ^0). At tree-level, the Higgs self-coupling is related to its mass. If λ is the quartic Higgs self-interaction strength [see eq. (47)], then $\lambda = m_{\phi^0}^2/v^2$. This means that one cannot take m_{ϕ^0} arbitrarily large without the attendant growth in λ . That is, the heavy Higgs limit in the Standard Model exhibits non-decoupling. In models of a non-minimal Higgs sector, the situation is more complex. In some models (with the Standard Model as one example), it is not possible to take any Higgs mass much larger than $\mathcal{O}(v)$ without finding at least one strong Higgs self-coupling. In other models, one finds that the non-minimal Higgs boson masses can be taken large at fixed Higgs self-couplings. Such behavior can arise in models that possess one (or more) off-diagonal squared-mass parameters in addition to the diagonal scalar squared-masses. In the limit where the off-diagonal squared-mass parameters are taken large [keeping the dimensionless Higgs self-couplings fixed and $\lesssim \mathcal{O}(1)$], the heavy Higgs states decouple, while both light and heavy Higgs bosons remain weakly-coupled. In this decoupling limit, exactly one neutral CP-even Higgs scalar remains light, and its properties are precisely those of the (weakly-coupled) Standard Model Higgs boson. That is, $h^0 \simeq \phi^0$, with

$m_{h^0} \sim \mathcal{O}(m_Z)$, and all other non-minimal Higgs states are significantly heavier than m_{h^0} . Squared-mass splittings of the heavy Higgs states are of $\mathcal{O}(m_Z^2)$, which means that all heavy Higgs states are approximately degenerate, with mass differences of order m_Z^2/m_{A^0} (here m_{A^0} is approximately equal to the common heavy Higgs mass scale). In contrast, if the non-minimal Higgs sector is weakly coupled but far from the decoupling limit, then h^0 is not separated in mass from the other Higgs states. In this case, the properties² of h^0 differ significantly from those of ϕ^0 .

Below, I exhibit the decoupling limit of the most general CP-even two-Higgs-doublet model [13]. It is convenient to define four squared mass combinations:

$$\begin{aligned} m_L^2 &\equiv \mathcal{M}_{11}^2 \cos^2 \beta + \mathcal{M}_{22}^2 \sin^2 \beta + \mathcal{M}_{12}^2 \sin 2\beta, \\ m_D^2 &\equiv \left(\mathcal{M}_{11}^2 \mathcal{M}_{22}^2 - \mathcal{M}_{12}^4 \right)^{1/2}, \\ m_T^2 &\equiv \mathcal{M}_{11}^2 + \mathcal{M}_{22}^2, \\ m_S^2 &\equiv m_{A^0}^2 + m_T^2, \end{aligned} \tag{17}$$

in terms of the elements of the neutral CP-even Higgs squared-mass matrix [eq. (5)]. In terms of the above quantities,

$$m_{H^0, h^0}^2 = \frac{1}{2} \left[m_S^2 \pm \sqrt{m_S^4 - 4m_{A^0}^2 m_L^2 - 4m_D^4} \right], \tag{18}$$

and

$$\cos^2(\beta - \alpha) = \frac{m_L^2 - m_{h^0}^2}{m_{H^0}^2 - m_{h^0}^2}. \tag{19}$$

In the decoupling limit, all the Higgs self-coupling constants λ_i are held fixed such that $\lambda_i \lesssim 1$, while taking $m_{A^0}^2 \gg \lambda_i v^2$. Then $\mathcal{M}_{ij}^2 \sim \mathcal{O}(v^2)$, and it follows that:

$$m_{h^0} \simeq m_L, \quad m_{H^0} \simeq m_{A^0} \simeq m_{H^\pm}, \tag{20}$$

and

$$\cos^2(\beta - \alpha) \simeq \frac{m_L^2(m_T^2 - m_L^2) - m_D^4}{m_{A^0}^4}. \tag{21}$$

Note that eq. (21) implies that $\cos(\beta - \alpha) = \mathcal{O}(m_Z^2/m_{A^0}^2)$ in the decoupling limit, which means that the h^0 couplings to Standard Model particles match precisely those of the Standard Model Higgs boson. These results are easily confirmed by considering the $\cos(\beta - \alpha) \rightarrow 0$ limit of eqs. (9)–(15).

²The basic property of the Higgs coupling strength proportional to mass is maintained. But, the precise coupling strength patterns of h^0 will differ from those of ϕ^0 in the non-decoupling limit.

Although no experimental evidence for the Higgs boson yet exists, there are some experimental as well as theoretical constraints on the parameters of the two-Higgs doublet model. Experimental limits on the charged and neutral Higgs masses have been obtained at LEP. For the charged Higgs boson, $m_{H^\pm} > 44$ GeV [14]. This is the most model-independent bound and assumes only that the H^\pm decays dominantly into $\tau^+\nu_\tau$, $c\bar{s}$ and $c\bar{b}$. The LEP limits on the masses of h^0 and A^0 are obtained by searching simultaneously for $e^+e^- \rightarrow h^0 f \bar{f}$ and $e^+e^- \rightarrow h^0 A^0$, which are mediated by s -channel Z -exchange [15]. The ZZh^0 and $Zh^0 A^0$ couplings that govern these two decay rates are proportional to $\sin(\beta - \alpha)$ and $\cos(\beta - \alpha)$, respectively. Thus, one can use the LEP data to deduce limits on m_{h^0} and m_{A^0} as a function of $\sin(\beta - \alpha)$. Stronger limits can be obtained in the MSSM where $\sin(\beta - \alpha)$ is determined by other model parameters. At present, taking into account data from LEP-1 and the most recent LEP-2 data (at $\sqrt{s} = 161$ and 172 GeV), one can exclude the MSSM Higgs mass ranges: $m_{h^0} < 62.5$ GeV (independent of the value of $\tan\beta$) and $m_{A^0} < 62.5$ GeV (assuming $\tan\beta > 1$) [16].

The experimental information on the parameter $\tan\beta$ is quite meager. For definiteness, let us assume that the Higgs-fermion couplings are specified as in eq. (15). The Higgs coupling to top quarks is proportional to $gm_t/2m_W$, and is therefore the strongest of all Higgs-fermion couplings. For $\tan\beta < 1$, the Higgs couplings to top-quarks are further enhanced by a factor of $1/\tan\beta$. As a result, some experimental limits on $\tan\beta$ exist based on the non-observation of virtual effects involving the $H^- t \bar{b}$ coupling. Clearly, such limits depend both on m_{H^\pm} and $\tan\beta$. The most sensitive limits are obtained from the measurements of $B^0 - \bar{B}^0$ mixing and the widths of $b \rightarrow s\gamma$ and $Z \rightarrow b\bar{b}$ [17]. For example, the process $b \rightarrow s\gamma$ can be significantly enhanced due to charged Higgs boson exchange. If there are no other competing non-Standard Model contributions (and this is a big *if*), then present data excludes charged Higgs masses less than about 250 GeV [18] (independent of the value of $\tan\beta$). In some regions of $\tan\beta$, the limits on the charged Higgs mass can be even more severe. However, other virtual contributions may exist that can cancel the effects of the charged Higgs exchange. For example, in the MSSM, constraints on $\tan\beta$ and m_{H^\pm} are significantly weaker. For $\tan\beta \gg 1$, the Higgs couplings to bottom-quarks are enhanced by a factor of $\tan\beta$. In this case, the measured rate for the inclusive decay of $B \rightarrow X + \tau\nu_\tau$ can be used to set an upper limit on $\tan\beta$ as a function of the charged Higgs mass. This is accomplished by setting a limit on the contribution of the *tree-level* charged Higgs exchange. Present data can be used to set a 2σ upper bound of $\tan\beta < 42(m_{H^\pm}/m_W)$ [19]. In the MSSM, this bound could be weakened due to one-loop QCD corrections mediated by the exchange of supersymmetric particles [20].

Theoretical considerations also lead to bounds on $\tan\beta$. The crudest bounds arise from unitarity constraints. If $\tan\beta$ becomes too small, then the Higgs coupling to top quarks becomes too strong. In this case, the tree-unitarity of processes

involving the Higgs-top quark Yukawa coupling is violated. Perhaps this should not be regarded as a theoretical defect, although it does render any perturbative analysis unreliable. A rough lower bound advocated by Ref. [21], $\tan\beta \gtrsim 0.3$, corresponds to a Higgs-top quark coupling in the perturbative region. A similar argument involving the Higgs-bottom quark coupling would yield $\tan\beta \lesssim 120$. A more solid theoretical constraint is based on the requirement that Higgs-fermion Yukawa couplings remain finite when running from the electroweak scale to some large energy scale Λ . Above Λ , one assumes that new physics enters. The limits on $\tan\beta$ depend on m_t and the choice of the high energy scale Λ . Using the renormalization group equations given in Appendix B, one integrates from the electroweak scale to Λ (allowing for the possible existence of a supersymmetry-breaking scale, $m_Z \leq M_{\text{SUSY}} \leq \Lambda$), and determines the region of $\tan\beta$ - m_t parameter space in which the Higgs-fermion Yukawa couplings remain finite. This exercise has recently been carried out at two-loops in Ref. [22]. Suppose that the low-energy theory at the electroweak scale is the MSSM, and that there is no additional new physics below the grand unification scale of $\Lambda = 2 \times 10^{16}$ GeV. Then, for $m_t = 170$ GeV, the Higgs-fermion Yukawa couplings remain finite at all energy scales below Λ if $1.5 \lesssim \tan\beta \lesssim 65$. Note that this result is consistent with the scenario of radiative electroweak symmetry breaking in low-energy supersymmetry based on supergravity, which requires that $1 \lesssim \tan\beta \lesssim m_t/m_b$.

3 The Higgs Sector of the MSSM at Tree Level

The Higgs sector of the MSSM is a CP-conserving two-Higgs-doublet model, with a Higgs potential whose dimension-four terms respect supersymmetry and with restricted Higgs-fermion couplings in which Φ_1 couples exclusively to down-type fermions while Φ_2 couples exclusively to up-type fermions [8]. Using the notation of eq. (1), the quartic couplings λ_i are given by

$$\begin{aligned}\lambda_1 &= \lambda_2 = \frac{1}{4}(g^2 + g'^2), \\ \lambda_3 &= \frac{1}{4}(g^2 - g'^2), \\ \lambda_4 &= -\frac{1}{2}g^2, \\ \lambda_5 &= \lambda_6 = \lambda_7 = 0.\end{aligned}\tag{22}$$

Inserting these results into eqs. (4) and (5), it follows that

$$\begin{aligned}m_{A^0}^2 &= m_{12}^2(\tan\beta + \cot\beta), \\ m_{H^\pm}^2 &= m_{A^0}^2 + m_W^2,\end{aligned}\tag{23}$$

and the tree-level neutral CP-even mass matrix is given by

$$\mathcal{M}_0^2 = \begin{pmatrix} m_{A^0}^2 \sin^2 \beta + m_Z^2 \cos^2 \beta & -(m_{A^0}^2 + m_Z^2) \sin \beta \cos \beta \\ -(m_{A^0}^2 + m_Z^2) \sin \beta \cos \beta & m_{A^0}^2 \cos^2 \beta + m_Z^2 \sin^2 \beta \end{pmatrix}. \quad (24)$$

The eigenvalues of \mathcal{M}_0^2 are the squared masses of the two CP-even Higgs scalars

$$m_{H^0, h^0}^2 = \frac{1}{2} \left(m_{A^0}^2 + m_Z^2 \pm \sqrt{(m_{A^0}^2 + m_Z^2)^2 - 4m_Z^2 m_{A^0}^2 \cos^2 2\beta} \right). \quad (25)$$

and the diagonalizing angle is α , with

$$\cos 2\alpha = -\cos 2\beta \left(\frac{m_{A^0}^2 - m_Z^2}{m_{H^0}^2 - m_{h^0}^2} \right), \quad \sin 2\alpha = -\sin 2\beta \left(\frac{m_{H^0}^2 + m_{h^0}^2}{m_{H^0}^2 - m_{h^0}^2} \right). \quad (26)$$

From these results, it is easy to obtain:

$$\cos^2(\beta - \alpha) = \frac{m_{h^0}^2(m_Z^2 - m_{h^0}^2)}{m_{A^0}^2(m_{H^0}^2 - m_{h^0}^2)}. \quad (27)$$

Thus, in the MSSM, two parameters (conveniently chosen to be m_{A^0} and $\tan \beta$) suffice to fix all other tree-level Higgs sector parameters.

Consider the decoupling limit where $m_{A^0} \gg m_Z$. Then, the above formulae yield

$$\begin{aligned} m_{h^0}^2 &\simeq m_Z^2 \cos^2 2\beta, \\ m_{H^0}^2 &\simeq m_{A^0}^2 + m_Z^2 \sin^2 2\beta, \\ m_{H^\pm}^2 &= m_{A^0}^2 + m_W^2, \\ \cos^2(\beta - \alpha) &\simeq \frac{m_Z^4 \sin^2 4\beta}{4m_{A^0}^4}. \end{aligned} \quad (28)$$

Two consequences are immediately apparent. First, $m_{A^0} \simeq m_{H^0} \simeq m_{H^\pm}$, up to corrections of $\mathcal{O}(m_Z^2/m_{A^0})$. Second, $\cos(\beta - \alpha) = 0$ up to corrections of $\mathcal{O}(m_Z^2/m_{A^0}^2)$. Of course, these results were expected based on the discussion of the decoupling limit in the general two-Higgs-doublet model given in section 2.

Finally, a number of important mass inequalities can be derived from the expressions for the tree-level Higgs masses obtained above,

$$\begin{aligned} m_{h^0} &\leq m_{A^0} \\ m_{h^0} &\leq m|\cos 2\beta| \leq m_Z, \quad \text{with } m \equiv \min(m_Z, m_{A^0}) \\ m_{H^0} &\geq m_Z, \\ m_{H^\pm} &\geq m_W. \end{aligned} \quad (29)$$

4 Radiative Corrections to the MSSM Higgs Masses

4.1 Overview

The tree-level results of the previous section are modified when radiative corrections are incorporated. Naively, one might expect radiative corrections to have a minor effect on the phenomenological implications of the model. However, in the MSSM, some of the tree-level Higgs mass relations may be significantly changed at one-loop, with profound implications for the phenomenology. For example, consider the tree-level bound on the lightest CP-even Higgs boson of the MSSM: $m_{h^0} \leq m_Z |\cos 2\beta| \leq m_Z$. The LEP-2 collider (running at its projected maximum center-of-mass energy of 192 GeV, with an integrated luminosity of 150 pb^{-1}) will discover at least one Higgs boson of the MSSM if $m_{h^0} \leq m_Z$ [15]. Thus, if the tree-level Higgs mass bound holds, then the absence of a Higgs discovery at LEP would rule out the MSSM. However, when radiative corrections are included, the light Higgs mass upper bound may be increased significantly. In the one-loop leading logarithmic approximation [23,24]

$$m_{h^0}^2 \lesssim m_Z^2 \cos^2 \beta + \frac{3g^2 m_t^4}{8\pi^2 m_W^2} \ln \left(\frac{M_{\tilde{t}_1} M_{\tilde{t}_2}}{m_t^2} \right), \quad (30)$$

where $M_{\tilde{t}_1}$, $M_{\tilde{t}_2}$ are the masses of the two top-squark mass eigenstates. Observe that the Higgs mass upper bound is very sensitive to the top mass and depends logarithmically on the top-squark masses. In addition, due to the increased upper bound for m_{h^0} , the non-observation of a Higgs boson at LEP-2 cannot rule out the MSSM.

Although eq. (30) provides a rough guide to the Higgs mass upper bound, it is not sufficiently precise for LEP-2 phenomenology, whose Higgs mass reach depends delicately on the MSSM parameters. In addition, in order to perform precision Higgs measurements and make comparisons with theory, more accurate results for the Higgs sector masses (and couplings) are required. The radiative corrections to the Higgs mass have been computed by a number of techniques, and using a variety of approximations such as effective potential [24,25,26,27,28] and diagrammatic methods [23,29,30,31,32,33,34]. Complete one-loop diagrammatic computations of the MSSM Higgs masses have been presented by a number of groups [34]; the resulting expressions are quite complex, and depend on all the parameters of the MSSM. (The dominant two-loop next-to-leading logarithmic results are also known [33].) Moreover, as noted above, the largest contribution to the one-loop radiative corrections is enhanced by a factor of m_t^4 and grows logarithmically with the top squark mass. Thus, higher order radiative corrections can be non-negligible for large top squark masses, in which case the large logarithms must be resummed.

The renormalization group (RG) techniques for resumming the leading logarithms has been developed by a number of authors [35,36,37]. The computation of the RG-improved one-loop corrections requires numerical integration of a coupled set of RG equations [37]. Although this program has been carried out in the literature, the procedure is unwieldy and not easily amenable to large-scale Monte-Carlo analyses. Recently, two groups have presented a simple analytic procedure for accurately approximating m_{h^0} . These methods can be easily implemented, and incorporate both the leading one-loop and two-loop effects and the RG-improvement. Also included are the leading effects at one loop of the supersymmetric thresholds (the most important effects of this type are squark mixing effects in the third generation). Details of the techniques can be found in Refs. [38] and [28]. Here, I simply quote two specific bounds, assuming $m_t = 175$ GeV and $M_{\tilde{t}} \lesssim 1$ TeV: $m_{h^0} \lesssim 112$ GeV if top-squark mixing is negligible, while $m_{h^0} \lesssim 125$ GeV if top-squark mixing is “maximal”. Maximal mixing corresponds to an off-diagonal squark squared-mass that produces the largest value of m_{h^0} . This mixing leads to an extremely large splitting of top-squark mass eigenstates.

The charged Higgs mass is also constrained in the MSSM. At tree level, m_{H^\pm} is given by eq. (23), which implies that charged Higgs bosons cannot be pair produced at LEP-2. Radiative corrections modify the tree-level prediction, but the corrections are typically smaller than the neutral Higgs mass corrections discussed above. Although $m_{H^\pm} \geq m_W$ is not a strict bound when one-loop corrections are included, the bound holds approximately over most of MSSM parameter space (and can be significantly violated only when $\tan \beta$ is well below 1, a region of parameter space that is theoretically disfavored).

In the remainder of this section, I shall present formulae which exhibit the leading contributions to the one-loop corrected Higgs masses. Symbolically,

$$\begin{aligned} m_{H^\pm}^2 &= (m_{H^\pm}^2)_{\text{1LL}} + (\Delta m_{H^\pm}^2)_{\text{mix}} , \\ \mathcal{M}^2 &= \mathcal{M}_{\text{1LL}}^2 + \Delta \mathcal{M}_{\text{mix}}^2 , \end{aligned} \tag{31}$$

where the subscript *1LL* refers to the tree-level plus the one-loop leading logarithmic approximation to the full one-loop calculation, and the subscript *mix* refers to the contributions arising from \tilde{q}_L - \tilde{q}_R mixing effects of the third generation squarks. The CP-even Higgs mass-squared eigenvalues are then obtained by using eq. (7) and the corresponding mixing angle, α , is obtained from eq. (8).

In the simplest approximation, squark mixing effects are neglected and the supersymmetric spectrum is characterized by one scale, called M_{SUSY} . We assume that M_{SUSY} is sufficiently large compared to m_Z such that logarithmically enhanced terms at one-loop dominate over the non-logarithmic terms.³ In this case, the

³If this condition does not hold, then the radiative corrections would constitute only a minor perturbation on the tree-level predictions.

full one-loop corrections (*e.g.*, obtained by a diagrammatic computation) are well approximated by the one-loop leading logarithmic approximation. Next, we incorporate the effects of squark mixing, which constitute the largest potential source of non-logarithmic one-loop corrections. In particular, these contributions to the Higgs mass radiative corrections arise from the exchange of the third generation squarks. Now, the approximation is parameterized by four supersymmetric parameters: M_{SUSY} (a common supersymmetric particle mass) and the third generation squark mixing parameters: A_t , A_b and μ . A more comprehensive set of formulae can be derived by treating the third generation squark sector more precisely by accounting for non-degenerate top and bottom squark masses. This approximation is characterized by seven supersymmetric parameters—the three squark mixing parameters mentioned above, three soft-supersymmetry-breaking diagonal squark mass parameters, M_Q , M_U , and M_D , and a common supersymmetry mass parameter M_{SUSY} which characterizes the masses of the first two generations of squarks, the sleptons, the charginos, and the neutralinos.

Given an approximation to the one-loop Higgs mass (at some level of approximation as described above), one must incorporate the RG-improvement if $M_{\text{SUSY}} \gg m_Z$. A simple analytic procedure of Ref. [38] is described in the section 5, and some numerical results are presented there. Similar results have also been obtained by Carena and collaborators, where analytic approximations to the RG-improved radiatively corrected MSSM Higgs masses are also developed [28]. Although the approaches are somewhat different, the numerical results (in cases which have been compared) typically agree to within 1 GeV in the evaluation of Higgs masses.

4.2 One-Loop Leading Logarithmic Corrections to the MSSM Higgs Masses

The leading logarithmic expressions for Higgs masses can be computed from the one-loop renormalization group equations (RGEs) of the gauge and Higgs self-couplings, following Ref. [37]. The method employs eqs. (4) and (5), which are evaluated by treating the λ_i as running parameters evaluated at the electroweak scale, M_{weak} . In addition, we identify the W and Z masses by

$$\begin{aligned} m_W^2 &= \frac{1}{4}g^2(v_1^2 + v_2^2), \\ m_Z^2 &= \frac{1}{4}(g^2 + g'^2)(v_1^2 + v_2^2), \end{aligned} \tag{32}$$

where the running gauge couplings are also evaluated at M_{weak} . Of course, the gauge couplings, g and g' are known from experimental measurements which are performed at the scale M_{weak} . The $\lambda_i(M_{\text{weak}}^2)$ are determined from supersymmetric boundary conditions at M_{SUSY} and RGE running down to M_{weak} . That is, if

supersymmetry were unbroken, then the λ_i would be fixed according to eq. (22). Since supersymmetry is broken, we regard eq. (22) as boundary conditions for the running parameters, valid at (and above) the energy scale M_{SUSY} . That is, we take

$$\begin{aligned}\lambda_1(M_{\text{SUSY}}^2) &= \lambda_2(M_{\text{SUSY}}^2) = \frac{1}{4}[g^2(M_{\text{SUSY}}^2) + g'^2(M_{\text{SUSY}}^2)], \\ \lambda_3(M_{\text{SUSY}}^2) &= \frac{1}{4} \left[g^2(M_{\text{SUSY}}^2) - g'^2(M_{\text{SUSY}}^2) \right], \\ \lambda_4(M_{\text{SUSY}}^2) &= -\frac{1}{2}g^2(M_{\text{SUSY}}^2), \\ \lambda_5(M_{\text{SUSY}}^2) &= \lambda_6(M_{\text{SUSY}}^2) = \lambda_7(M_{\text{SUSY}}^2) = 0,\end{aligned}\tag{33}$$

in accordance with the tree-level relations of the MSSM. At scales below M_{SUSY} , the gauge and quartic couplings evolve according to the renormalization group equations (RGEs) of the non-supersymmetric two-Higgs-doublet model given in eqs. (B.5)–(B.7). These equations are of the form:

$$\frac{dp_i}{dt} = \beta_i(p_1, p_2, \dots) \quad \text{with } t \equiv \ln \mu^2,\tag{34}$$

where μ is the energy scale, and the p_i are the parameters of the theory ($p_i = g_j^2, \lambda_k, \dots$). The relevant β -functions can be found in Appendix B. The boundary conditions together with the RGEs imply that, at the leading-log level, λ_5 , λ_6 and λ_7 are zero at all energy scales. Solving the RGEs with the supersymmetric boundary conditions at M_{SUSY} , one can determine the λ_i at the weak scale. The resulting values for $\lambda_i(M_{\text{weak}})$ are then inserted into eqs. (4) and (5) to obtain the radiatively corrected Higgs masses. Having solved the one-loop RGEs, the Higgs masses thus obtained include the leading logarithmic radiative corrections summed to all orders in perturbation theory.

The RGEs can be solved by numerical analysis on the computer. In order to derive the one-loop leading logarithmic corrections, it is sufficient to solve the RGEs iteratively. In first approximation, we can take the right hand side of eq. (34) to be independent of μ^2 . That is, we compute the β_i by evaluating the parameters p_i at the scale $\mu = M_{\text{SUSY}}$. Then, integration of the RGEs is trivial, and we obtain

$$p_i(M_{\text{weak}}^2) = p_i(M_{\text{SUSY}}^2) - \beta_i \ln \left(\frac{M_{\text{SUSY}}^2}{M_{\text{weak}}^2} \right).\tag{35}$$

This result demonstrates that the first iteration corresponds to computing the one-loop radiative corrections in which only terms proportional to $\ln M_{\text{SUSY}}^2$ are kept. It is straightforward to work out the one-loop leading logarithmic expressions for the λ_i and the Higgs masses.

First consider the charged Higgs mass. Since $\lambda_5(\mu^2) = 0$ at all scales, we need only consider λ_4 . Evaluating β_{λ_4} at $\mu = M_{\text{SUSY}}$, we compute

$$\lambda_4(m_W^2) = -\frac{1}{2}g^2 - \frac{1}{32\pi^2} \left[\left(\frac{4}{3}N_g + \frac{1}{6}N_H - \frac{10}{3} \right) g^4 + 5g^2g'^2 - \frac{3g^4}{2m_W^2} \left(\frac{m_t^2}{s_\beta^2} + \frac{m_b^2}{c_\beta^2} \right) + \frac{3g^2m_t^2m_b^2}{s_\beta^2c_\beta^2m_W^4} \right] \ln \left(\frac{M_{\text{SUSY}}^2}{m_W^2} \right). \quad (36)$$

The terms proportional to the number of generations $N_g = 3$ and the number of Higgs doublets $N_H = 2$ that remain in the low-energy effective theory at the scale $\mu = m_W$ have their origin in the running of g^2 from M_{SUSY} down to m_W . In deriving this expression, I have taken $M_{\text{weak}} = m_W$. This is a somewhat arbitrary decision, since another reasonable choice would yield a result that differs from eq. (36) by a non-leading logarithmic term. Comparisons with a more complete calculation show that one should choose $M_{\text{weak}} = m_W$ in computations involving the charged Higgs (and gauge) sector, and $M_{\text{weak}} = m_Z$ in computations involving the neutral sector.

The above analysis also assumes that $m_t \sim \mathcal{O}(m_W)$. Although this is a good assumption, we can improve the above result somewhat by decoupling the (t, b) weak doublet from the low-energy theory for scales below m_t . The terms in eq. (36) that are proportional to m_t^2 and/or m_b^2 arise from self-energy diagrams containing a tb loop. Thus, such a term should not be present for $m_W \leq \mu \leq m_t$. In addition, we recognize the term in eq. (36) proportional to the number of generations N_g as arising from the contributions to the self-energy diagrams containing either quark or lepton loops (and their supersymmetric partners). To identify the contribution of the tb loop to this term, simply write

$$N_g = \frac{1}{4}N_g(N_c + 1) = \frac{1}{4}N_c + \frac{1}{4}[N_c(N_g - 1) + N_g], \quad (37)$$

where $N_c = 3$ colors. Thus, we identify $\frac{1}{4}N_c$ as the piece of the term proportional to N_g that is due to the tb loop. The rest of this term is then attributed to the lighter quarks and leptons. Finally, the remaining terms in eq. (36) are due to the contributions from the gauge and Higgs boson sector. The final result is [31]

$$\lambda_4(m_W^2) = -\frac{1}{2}g^2 - \frac{N_cg^4}{32\pi^2} \left[\frac{1}{3} - \frac{1}{2m_W^2} \left(\frac{m_t^2}{s_\beta^2} + \frac{m_b^2}{c_\beta^2} \right) + \frac{m_t^2m_b^2}{s_\beta^2c_\beta^2m_W^4} \right] \ln \left(\frac{M_{\text{SUSY}}^2}{m_t^2} \right) - \frac{1}{96\pi^2} \left\{ [N_c(N_g - 1) + N_g + \frac{1}{2}N_H - 10] g^4 + 15g^2g'^2 \right\} \ln \left(\frac{M_{\text{SUSY}}^2}{m_W^2} \right). \quad (38)$$

Inserting this result (and $\lambda_5 = 0$) into eq. (4), we obtain the one-loop leading-logarithmic (1LL) formula for the charged Higgs mass

$$(m_{H^\pm}^2)_{1LL} = m_A^2 + m_W^2 + \frac{N_c g^2}{32\pi^2 m_W^2} \left[\frac{2m_t^2 m_b^2}{s_\beta^2 c_\beta^2} - m_W^2 \left(\frac{m_t^2}{s_\beta^2} + \frac{m_b^2}{c_\beta^2} \right) + \frac{2}{3} m_W^4 \right] \\ \times \ln \left(\frac{M_{\text{SUSY}}^2}{m_t^2} \right) + \frac{m_W^2}{48\pi^2} \{ [N_c(N_g - 1) + N_g - 9] g^2 + 15g'^2 \} \ln \left(\frac{M_{\text{SUSY}}^2}{m_W^2} \right). \quad (39)$$

Since this derivation makes use of the two-Higgs-doublet RGEs for the λ_i , there is an implicit assumption that the full two-doublet Higgs spectrum survives in the low-energy effective theory at $\mu = m_W$. Thus, I have set $N_H = 2$ in obtaining eq. (39) above. It also means that m_{A^0} cannot be much larger than m_W .⁴ The leading logarithms of eq. (39) can be resummed to all orders of perturbation theory by using the full RGE solution to $\lambda_4(m_W^2)$

$$m_{H^\pm}^2 = m_{A^0}^2 - \frac{1}{2} \lambda_4(m_W^2) (v_1^2 + v_2^2). \quad (40)$$

Although the one-loop leading-log formula for m_{H^\pm} [eq. (39)] gives a useful indication as to the size of the radiative corrections, non-leading logarithmic contributions can also be important in certain regions of parameter space. A more complete set of radiative corrections can be found in the literature [26,29,30,31,34]. However, it should be emphasized that the radiative corrections to the charged Higgs mass are significant only for $\tan\beta < 1$, a region of MSSM parameter space not favored in supersymmetric models.

The computation of the neutral CP-even Higgs masses follows a similar procedure. The results of Ref. [37] are summarized below. From eq. (5), we see that we only need results for λ_1 , λ_2 and $\tilde{\lambda}_3 \equiv \lambda_3 + \lambda_4 + \lambda_5$. (Recall that $\lambda_5 = \lambda_6 = \lambda_7 = 0$ at all energy scales.) By iterating the corresponding RGEs as before, we find

⁴If $m_{A^0} \sim \mathcal{O}(M_{\text{SUSY}})$, then H^\pm , H^0 and A^0 would all have masses of order M_{SUSY} , and the effective low-energy theory below M_{SUSY} would be that of the minimal Standard Model. For example, for $m_{A^0} = M_{\text{SUSY}}$, the leading logarithmic corrections to the charged Higgs mass can be obtained from $m_{H^\pm}^2 = m_{A^0}^2 + m_W^2$ by treating m_W^2 as a running parameter evaluated at m_{A^0} . Re-expressing $m_W(m_{A^0})$ in terms of the physical W mass yields the correct one-loop leading log correction to $m_{H^\pm}^2$. For $m_Z \leq m_{A^0} \leq M_{\text{SUSY}}$, one can interpolate between the effective two-Higgs doublet model and the effective one-Higgs doublet model.

$$\begin{aligned}
\lambda_1(m_Z^2) &= \frac{1}{4}[g^2 + g'^2](m_Z^2) + \frac{g^4}{384\pi^2 c_W^4} \left[P_t \ln \left(\frac{M_{\text{SUSY}}^2}{m_t^2} \right) \right. \\
&\quad \left. + \left(12N_c \frac{m_b^4}{m_Z^4 c_\beta^4} - 6N_c \frac{m_b^2}{m_Z^2 c_\beta^2} + P_b + P_f + P_g + P_{2H} \right) \ln \left(\frac{M_{\text{SUSY}}^2}{m_Z^2} \right) \right], \\
\lambda_2(m_Z^2) &= \frac{1}{4}[g^2 + g'^2](m_Z^2) + \frac{g^4}{384\pi^2 c_W^4} \left[\left(P_b + P_f + P_g + P_{2H} \right) \ln \left(\frac{M_{\text{SUSY}}^2}{m_Z^2} \right) \right. \\
&\quad \left. + \left(12N_c \frac{m_t^4}{m_Z^4 s_\beta^4} - 6N_c \frac{m_t^2}{m_Z^2 s_\beta^2} + P_t \right) \ln \left(\frac{M_{\text{SUSY}}^2}{m_t^2} \right) \right], \\
\tilde{\lambda}_3(m_Z^2) &= -\frac{1}{4}[g^2 + g'^2](m_Z^2) - \frac{g^4}{384\pi^2 c_W^4} \left[\left(P_t - 3N_c \frac{m_t^2}{m_Z^2 s_\beta^2} \right) \ln \left(\frac{M_{\text{SUSY}}^2}{m_t^2} \right) \right. \\
&\quad \left. + \left(-3N_c \frac{m_b^2}{m_Z^2 c_\beta^2} + P_b + P_f + P'_g + P'_{2H} \right) \ln \left(\frac{M_{\text{SUSY}}^2}{m_Z^2} \right) \right], \tag{41}
\end{aligned}$$

where

$$\begin{aligned}
P_t &\equiv N_c(1 - 4e_t s_W^2 + 8e_t^2 s_W^4), \\
P_b &\equiv N_c(1 + 4e_b s_W^2 + 8e_b^2 s_W^4), \\
P_f &\equiv N_c(N_g - 1)[2 - 4s_W^2 + 8(e_t^2 + e_b^2)s_W^4] + N_g[2 - 4s_W^2 + 8s_W^4], \\
P_g &\equiv -44 + 106s_W^2 - 62s_W^4, \\
P'_g &\equiv 10 + 34s_W^2 - 26s_W^4, \\
P_{2H} &\equiv -10 + 2s_W^2 - 2s_W^4, \\
P'_{2H} &\equiv 8 - 22s_W^2 + 10s_W^4. \tag{42}
\end{aligned}$$

In the above formulae, the electric charges of the quarks are $e_t = 2/3$, $e_b = -1/3$, and the subscripts t, b, f, g and $2H$ indicate that these are the contributions from the top and bottom quarks, the other fermions (leptons and the first two generations of quarks), the gauge bosons and the Higgs doublets, and the corresponding supersymmetric partners, respectively.

As in the derivation of $\lambda_4(m_W^2)$ above, we have improved our analysis by removing the effects of top-quark loops below $\mu = m_t$. This requires a careful treatment of the evolution of g and g' at scales below $\mu = m_t$. The correct procedure is

somewhat subtle, since the full electroweak gauge symmetry is broken below top-quark threshold; for further details, see Ref. [37]. However, the following pedestrian technique works: consider the RGE for $g^2 + g'^2$ valid for $\mu < M_{\text{SUSY}}$

$$\frac{d}{dt}(g^2 + g'^2) = \frac{1}{96\pi^2} \left[\left(8g^4 + \frac{40}{3}g'^4\right) N_g + (g^4 + g'^4)N_H - 44g^4 \right]. \quad (43)$$

This equation is used to run $g^2 + g'^2$, which appears in eq. (33), from M_{SUSY} down to m_Z . As before, we identify the term proportional to N_g as corresponding to the fermion loops. We can explicitly extract the t -quark contribution by noting that

$$\begin{aligned} N_g \left(8g^4 + \frac{40}{3}g'^4\right) &= \frac{g^4 N_g}{c_W^4} \left[\frac{64}{3}s_W^4 - 16s_W^2 + 8 \right] \\ &= \frac{g^4}{c_W^4} \left\{ N_c [1 + (N_g - 1)] (1 - 4e_t s_W^2 + 8e_t^2 s_W^4) \right. \\ &\quad \left. + N_c N_g (1 + 4e_b s_W^2 + 8e_b^2 s_W^4) + N_g (2 - 4s_W^2 + 8s_W^4) \right\}, \end{aligned} \quad (44)$$

where in the first line of the last expression, the term proportional to 1 corresponds to the t -quark contribution while the term proportional to $N_g - 1$ accounts for the u and c -quarks; the second line contains the contributions from the down-type quarks and leptons respectively. Thus, iterating to one-loop,

$$\begin{aligned} [g^2 + g'^2](M_{\text{SUSY}}^2) &= [g^2 + g'^2](m_Z^2) + \frac{g^4}{96\pi^2 c_W^4} \left[P_t \ln \left(\frac{M_{\text{SUSY}}^2}{m_t^2} \right) \right. \\ &\quad \left. + [P_b + P_f + (s_W^4 + c_W^4)N_H - 44c_W^4] \ln \left(\frac{M_{\text{SUSY}}^2}{m_Z^2} \right) \right]. \end{aligned} \quad (45)$$

Again, we take $N_H = 2$, since the low-energy effective theory between m_Z and M_{SUSY} consists of the full two-Higgs doublet model. Eq. (45) was used in the derivation of eq. (41).

We now return to the computation of the one-loop leading log neutral CP-even Higgs squared-mass matrix. The final step is to insert the expressions obtained in eq. (41) into eq. (5). The resulting matrix elements for the mass-squared matrix to one-loop leading logarithmic accuracy are given by

$$\begin{aligned}
(\mathcal{M}_{11}^2)_{\text{1LL}} &= m_{A^0}^2 s_\beta^2 + m_Z^2 c_\beta^2 + \frac{g^2 m_Z^2 c_\beta^2}{96\pi^2 c_W^2} \left[P_t \ln \left(\frac{M_{\text{SUSY}}^2}{m_t^2} \right) \right. \\
&\quad \left. + \left(12N_c \frac{m_b^4}{m_Z^4 c_\beta^4} - 6N_c \frac{m_b^2}{m_Z^2 c_\beta^2} + P_b + P_f + P_g + P_{2H} \right) \ln \left(\frac{M_{\text{SUSY}}^2}{m_Z^2} \right) \right] \\
(\mathcal{M}_{22}^2)_{\text{1LL}} &= m_{A^0}^2 c_\beta^2 + m_Z^2 s_\beta^2 + \frac{g^2 m_Z^2 s_\beta^2}{96\pi^2 c_W^2} \left[\left(P_b + P_f + P_g + P_{2H} \right) \ln \left(\frac{M_{\text{SUSY}}^2}{m_Z^2} \right) \right. \\
&\quad \left. + \left(12N_c \frac{m_t^4}{m_Z^4 s_\beta^4} - 6N_c \frac{m_t^2}{m_Z^2 s_\beta^2} + P_t \right) \ln \left(\frac{M_{\text{SUSY}}^2}{m_t^2} \right) \right] \\
(\mathcal{M}_{12}^2)_{\text{1LL}} &= -s_\beta c_\beta \left\{ m_{A^0}^2 + m_Z^2 + \frac{g^2 m_Z^2}{96\pi^2 c_W^2} \left[\left(P_t - 3N_c \frac{m_t^2}{m_Z^2 s_\beta^2} \right) \ln \left(\frac{M_{\text{SUSY}}^2}{m_t^2} \right) \right. \right. \\
&\quad \left. \left. + \left(-3N_c \frac{m_b^2}{m_Z^2 c_\beta^2} + P_b + P_f + P'_g + P'_{2H} \right) \ln \left(\frac{M_{\text{SUSY}}^2}{m_Z^2} \right) \right] \right\}, \quad (46)
\end{aligned}$$

Diagonalizing this matrix [eq. (46)] yields the radiatively corrected CP-even Higgs masses and mixing angle α .

The analysis presented above assumes that m_{A^0} is not much larger than $\mathcal{O}(m_Z)$ so that the Higgs sector of the low-energy effective theory contains the full two-Higgs-doublet spectrum. On the other hand, if $m_{A^0} \gg m_Z$, then only h^0 remains in the low-energy theory. In this case, we must integrate out the heavy Higgs doublet, in which case one of the mass eigenvalues of \mathcal{M}_0^2 [eq. (24)] is much larger than the weak scale. In order to obtain the effective Lagrangian at M_{weak} , we first have to run the various coupling constants to the threshold m_{A^0} . Then we diagonalize the Higgs mass matrix and express the Lagrangian in terms of the mass eigenstates. Notice that in this case the mass eigenstate h^0 is directly related to the field with the non-zero vacuum expectation value [*i.e.*, $\beta(m_{A^0}) = \alpha(m_{A^0}) + \pi/2 + \mathcal{O}(m_Z^2/m_{A^0}^2)$].

Below m_{A^0} only the Standard Model Higgs doublet $\phi \equiv c_\beta \Phi_1 + s_\beta \Phi_2$ remains. The scalar potential is

$$\mathcal{V} = m_\phi^2 (\phi^\dagger \phi) + \frac{1}{2} \lambda (\phi^\dagger \phi)^2, \quad (47)$$

and the light CP-even Higgs mass is obtained using $m_{h^0}^2 = \lambda v^2$. The RGE in the Standard Model for λ is [39,40]

$$16\pi^2 \beta_\lambda = 6\lambda^2 + \frac{3}{8} [2g^4 + (g^2 + g'^2)^2] - 2 \sum_i N_{c_i} h_{f_i}^4 - \lambda \left(\frac{9}{2} g^2 + \frac{3}{2} g'^2 - 2 \sum_i N_{c_i} h_{f_i}^2 \right), \quad (48)$$

where the summation is over all fermions with $h_{f_i} = gm_{f_i}/(\sqrt{2}m_W)$. The RGEs for the gauge couplings are obtained from β_{g^2} and $\beta_{g'^2}$ given in Appendix B by putting $N_H = 1$. In addition, we require the boundary condition for λ at m_{A^0}

$$\begin{aligned}\lambda(m_{A^0}) &= \left[c_\beta^4 \lambda_1 + s_\beta^4 \lambda_2 + 2s_\beta^2 c_\beta^2 (\lambda_3 + \lambda_4 + \lambda_5) + 4c_\beta^3 s_\beta \lambda_6 + 4c_\beta s_\beta^3 \lambda_7 \right] (m_{A^0}) \\ &= \left[\frac{1}{4}(g^2 + g'^2) c_{2\beta}^2 \right] (m_{A^0}) + \frac{g^4}{384\pi^2 c_W^4} \ln \left(\frac{M_{\text{SUSY}}^2}{m_{A^0}^2} \right) \\ &\quad \times \left[12N_c \left(\frac{m_t^4}{m_Z^4} + \frac{m_b^4}{m_Z^4} \right) + 6N_c c_{2\beta} \left(\frac{m_t^2}{m_Z^2} - \frac{m_b^2}{m_Z^2} \right) \right. \\ &\quad \left. + c_{2\beta}^2 (P_t + P_b + P_f) + (s_\beta^4 + c_\beta^4) (P_g + P_{2H}) - 2s_\beta^2 c_\beta^2 (P'_g + P'_{2H}) \right], \quad (49)\end{aligned}$$

where $(g^2 + g'^2) c_{2\beta}^2$ is to be evaluated at the scale m_{A^0} as indicated. The RGE for $g^2 + g'^2$ was given in eq. (43); note that at scales below m_A we must set $N_H = 1$.

Finally, we must deal with implicit scale dependence of $c_{2\beta}^2$. Since the fields Φ_i ($i = 1, 2$) change with the scale, it follows that $\tan \beta$ scales like the ratio of the two Higgs doublet fields, *i.e.*,

$$\frac{1}{\tan^2 \beta} \frac{d \tan^2 \beta}{dt} = \frac{\Phi_1^2}{\Phi_2^2} \frac{d}{dt} \left(\frac{\Phi_2^2}{\Phi_1^2} \right) = \gamma_2 - \gamma_1. \quad (50)$$

Thus we arrive at the RGE for $\cos 2\beta$ in terms of the anomalous dimensions γ_i given in eq. (B.6). Solving this equation iteratively to first order yields

$$c_{2\beta}^2(m_{A^0}) = c_{2\beta}^2(m_Z) + 4c_{2\beta} c_\beta^2 s_\beta^2 (\gamma_1 - \gamma_2) \ln \left(\frac{m_{A^0}^2}{m_Z^2} \right). \quad (51)$$

The one loop leading log expression for $m_{h^0}^2 = \lambda(m_Z) v^2$ can now be obtained by solving the RGEs above for $\lambda(m_Z)$ iteratively to first order using the boundary condition given in eq. (49). The result is

$$\begin{aligned}(m_{h^0}^2)_{\text{1LL}} &= m_Z^2 c_{2\beta}^2(m_Z) + \frac{g^2 m_Z^2}{96\pi^2 c_W^2} \left\{ \left[12N_c \frac{m_b^4}{m_Z^4} - 6N_c c_{2\beta} \frac{m_b^2}{m_Z^2} + c_{2\beta}^2 (P_b + P_f) \right. \right. \\ &\quad \left. \left. + (P_g + P_{2H})(s_\beta^4 + c_\beta^4) - 2s_\beta^2 c_\beta^2 (P'_g + P'_{2H}) \right] \ln \left(\frac{M_{\text{SUSY}}^2}{m_Z^2} \right) \right. \\ &\quad \left. + \left[12N_c \frac{m_t^4}{m_Z^4} + 6N_c c_{2\beta} \frac{m_t^2}{m_Z^2} + c_{2\beta}^2 P_t \right] \ln \left(\frac{M_{\text{SUSY}}^2}{m_t^2} \right) \right. \\ &\quad \left. - \left[(c_\beta^4 + s_\beta^4) P_{2H} - 2c_\beta^2 s_\beta^2 P'_{2H} - P_{1H} \right] \ln \left(\frac{m_{A^0}^2}{m_Z^2} \right) \right\}, \quad (52)\end{aligned}$$

where the term proportional to

$$P_{1H} \equiv -9c_{2\beta}^4 + (1 - 2s_W^2 + 2s_W^4)c_{2\beta}^2, \quad (53)$$

corresponds to the Higgs boson contribution in the one-Higgs-doublet model. The term in eq. (52) proportional to $\ln(m_{A^0}^2)$ accounts for the fact that there are two Higgs doublets present at a scale above m_{A^0} but only one Higgs doublet below m_{A^0} .

We can improve the above one-loop leading log formulae by reinterpreting the meaning of M_{SUSY} . For example, all terms proportional to $\ln(M_{\text{SUSY}}^2/m_t^2)$ arise from diagrams with loops involving the top quark and top-squarks. Explicit diagrammatic computations then show that we can reinterpret $M_{\text{SUSY}}^2 = M_{\tilde{t}_1} M_{\tilde{t}_2}$. Note that with this reinterpretation of M_{SUSY}^2 , the top quark and top squark loop contributions to the Higgs masses cancel exactly when $M_{\tilde{t}_1} = M_{\tilde{t}_2} = m_t$, as required in the supersymmetric limit. Likewise, in terms proportional to P_b or powers of m_b multiplied by $\ln(M_{\text{SUSY}}^2/m_Z^2)$, we may reinterpret $M_{\text{SUSY}} = M_{\tilde{b}_1} M_{\tilde{b}_2}$. Terms proportional to $P_f \ln(M_{\text{SUSY}}^2/m_Z^2)$ come from loops of lighter quarks and leptons (and their supersymmetric partners) in an obvious way, and the corresponding M_{SUSY}^2 can be reinterpreted accordingly. The remaining leading logarithmic terms arise from gauge and Higgs boson loops and their supersymmetric partners. The best we can do in the above formulae is to interpret M_{SUSY} as an average neutralino and chargino mass. To incorporate thresholds more precisely requires a more complicated version of eq. (46), which can be easily derived from formulae given in Ref. [37]. The explicit form of these threshold corrections can be found in Ref. [38]. However, the impact of these corrections are no more important than the non-leading logarithmic terms which have been discarded.

The largest of the non-leading logarithmic terms is of $\mathcal{O}(g^2 m_t^2)$, which can be identified from a full one-loop computation as being the subdominant term relative to the leading $\mathcal{O}(g^2 m_t^4 \ln M_{\text{SUSY}}^2)$ term in \mathcal{M}_{22}^2 . Thus, we can make a minor improvement on our computation of the one-loop leading-log CP-even Higgs squared mass matrix by taking

$$\mathcal{M}^2 = \mathcal{M}_{\text{1LL}}^2 + \frac{N_c g^2 m_t^2}{48\pi^2 s_\beta^2 c_W^2} \begin{pmatrix} 0 & 0 \\ 0 & 1 \end{pmatrix}. \quad (54)$$

where $\mathcal{M}_{\text{1LL}}^2$ is the matrix whose elements are given in eq. (46). One can check that this yields at most a 1 GeV shift in the computed Higgs masses.

4.3 Leading Squark Mixing Corrections to the MSSM Higgs Masses

In the case of multiple and widely separated supersymmetric particle thresholds and/or large squark mixing (which is most likely in the top squark sector),

new non-leading logarithmic contributions to the scalar mass-squared matrix can become important. As shown in Ref. [37], such effects can be taken into account by modifying the boundary conditions of the λ_i at the supersymmetry breaking scale [eq. (33)], and by modifying the RGEs to account for multiple thresholds. In particular, we find that λ_5 , λ_6 and λ_7 are no longer zero. If the new RGEs are solved iteratively to one loop, then the effects of the new boundary conditions are simply additive.

In this section, we focus on the effects arising from the mass splittings and \tilde{q}_L – \tilde{q}_R mixing in the third generation squark sector. The latter generates additional squared-mass shifts proportional to m_t^4 and thus can have a significant impact on the radiatively corrected Higgs masses [27]. First, we define our notation (we follow the conventions of Ref. [7]). In third family notation, the squark mass eigenstates are obtained by diagonalizing the following two 2×2 matrices. The top-squark squared-masses are eigenvalues of

$$\begin{pmatrix} M_Q^2 + m_t^2 + t_L m_Z^2 & m_t X_t \\ m_t X_t & M_U^2 + m_t^2 + t_R m_Z^2 \end{pmatrix}, \quad (55)$$

where $X_t \equiv A_t - \mu \cot \beta$, $t_L \equiv (\frac{1}{2} - e_t \sin^2 \theta_W) \cos 2\beta$ and $t_R \equiv e_t \sin^2 \theta_W \cos 2\beta$. The bottom-squark squared-masses are eigenvalues of

$$\begin{pmatrix} M_Q^2 + m_b^2 + b_L m_Z^2 & m_b X_b \\ m_b X_b & M_D^2 + m_b^2 + b_R m_Z^2 \end{pmatrix}, \quad (56)$$

where $X_b \equiv A_b - \mu \tan \beta$, $b_L \equiv (-\frac{1}{2} - e_b \sin^2 \theta_W) \cos 2\beta$ and $b_R \equiv e_b \sin^2 \theta_W \cos 2\beta$. M_Q , M_U , M_D , A_t , and A_b are soft-supersymmetry-breaking parameters, and μ is the supersymmetric Higgs mass parameter. We treat the squark mixing perturbatively, assuming that the off-diagonal mixing terms are small compared to the diagonal terms.

At one-loop, the effect of the squark mixing is to introduce the shifts $\Delta \mathcal{M}_{\text{mix}}^2$ and $(\Delta m_{H^\pm}^2)_{\text{mix}}$. In order to keep the formulae simple, we take $M_Q = M_U = M_D = M_{\text{SUSY}}$, where M_{SUSY} is assumed to be large compared to m_Z . Thus, the radiatively corrected Higgs mass is determined by m_{A^0} , $\tan \beta$, M_{SUSY} , A_t , A_b , and μ . The more complex case of non-universal squark squared-masses (in which M_Q , M_U , and M_D are unequal but still large compared to m_Z) is treated in Ref. [38].

It is convenient to define

$$\begin{aligned} X_t &\equiv A_t - \mu \cot \beta, & Y_t &\equiv A_t + \mu \tan \beta, \\ X_b &\equiv A_b - \mu \tan \beta, & Y_b &\equiv A_b + \mu \cot \beta. \end{aligned} \quad (57)$$

We assume that the mixing terms $m_t X_t$ and $m_b X_b$ are not too large.⁵ Then, the

⁵Formally, the expressions given in eqs. (58)–(61) are the results of an expansion in the variable $(M_1^2 - M_2^2)/(M_1^2 + M_2^2)$, where M_1^2 , M_2^2 are the squared-mass eigenvalues of the squark mass matrix. Thus, we demand that $m_t X_t / M_{\text{SUSY}}^2 \ll 1$. For example, for $M_{\text{SUSY}} = 1$ TeV, values of $X_t / M_{\text{SUSY}} \lesssim 3$ should yield an acceptable approximation based on the formulae presented here.

elements of the CP-even Higgs squared-mass matrix are given by:

$$\mathcal{M}^2 = \mathcal{M}_{\text{1LL}}^2 + \Delta\mathcal{M}_{\text{mix}}^2, \quad (58)$$

where $\mathcal{M}_{\text{1LL}}^2$ has been given in eq. (46), and

$$\begin{aligned} (\Delta\mathcal{M}_{11}^2)_{\text{mix}} &= \frac{g^2 N_c}{32\pi^2 m_W^2 M_{\text{SUSY}}^2} \left[\frac{4m_b^4 A_b X_b}{\cos^2 \beta} \left(1 - \frac{A_b X_b}{12M_{\text{SUSY}}^2} \right) - \frac{m_t^4 \mu^2 X_t^2}{3M_{\text{SUSY}}^2 \sin^2 \beta} \right. \\ &\quad \left. - m_Z^2 m_b^2 A_b (X_b + \frac{1}{3}A_b) - m_Z^2 m_t^2 \mu \cot \beta (X_t + \frac{1}{3}\mu \cot \beta) \right], \\ (\Delta\mathcal{M}_{22}^2)_{\text{mix}} &= \frac{g^2 N_c}{32\pi^2 m_W^2 M_{\text{SUSY}}^2} \left[\frac{4m_t^4 A_t X_t}{\sin^2 \beta} \left(1 - \frac{A_t X_t}{12M_{\text{SUSY}}^2} \right) - \frac{m_b^4 \mu^2 X_b^2}{3M_{\text{SUSY}}^2 \cos^2 \beta} \right. \\ &\quad \left. - m_Z^2 m_t^2 A_t (X_t + \frac{1}{3}A_t) - m_Z^2 m_b^2 \mu \tan \beta (X_b + \frac{1}{3}\mu \tan \beta) \right], \\ (\Delta\mathcal{M}_{12}^2)_{\text{mix}} &= \frac{-g^2 N_c}{64\pi^2 m_W^2 M_{\text{SUSY}}^2} \left[\frac{4m_t^4 \mu X_t}{\sin^2 \beta} \left(1 - \frac{A_t X_t}{6M_{\text{SUSY}}^2} \right) + \frac{4m_b^4 \mu X_b}{\cos^2 \beta} \left(1 - \frac{A_b X_b}{6M_{\text{SUSY}}^2} \right) \right. \\ &\quad \left. - m_Z^2 m_t^2 \cot \beta \left[X_t Y_t + \frac{1}{3}(\mu^2 + A_t^2) \right] - m_Z^2 m_b^2 \tan \beta \left[X_b Y_b + \frac{1}{3}(\mu^2 + A_b^2) \right] \right]. \quad (59) \end{aligned}$$

If $m_Z \ll m_{A^0} \leq M_{\text{SUSY}}$, a separate analysis is required. One finds that eq. (52) is shifted by

$$\begin{aligned} (\Delta m_{h^0}^2)_{\text{mix}} &= \frac{g^2 N_c}{16\pi^2 m_W^2 M_{\text{SUSY}}^2} \left\{ 2m_t^4 X_t^2 \left(1 - \frac{X_t^2}{12M_{\text{SUSY}}^2} \right) + 2m_b^4 X_b^2 \left(1 - \frac{X_b^2}{12M_{\text{SUSY}}^2} \right) \right. \\ &\quad \left. + \frac{1}{2}m_Z^2 \cos 2\beta \left[m_t^2 \left(X_t^2 + \frac{1}{3}(A_t^2 - \mu^2 \cot^2 \beta) \right) - m_b^2 \left(X_b^2 + \frac{1}{3}(A_b^2 - \mu^2 \tan^2 \beta) \right) \right] \right\}. \quad (60) \end{aligned}$$

Squark mixing effects also lead to modifications of the charged Higgs squared-mass. One finds that the charged Higgs squared-mass obtained in eq. (39) is shifted by

$$\begin{aligned} (m_{H^\pm}^2)_{\text{mix}} &= \frac{N_c g^2}{192\pi^2 m_W^2 M_{\text{SUSY}}^2} \left[\frac{2m_t^2 m_W^2 (\mu^2 - 2A_t^2)}{\sin^2 \beta} + \frac{2m_b^2 m_W^2 (\mu^2 - 2A_b^2)}{\cos^2 \beta} \right. \\ &\quad \left. - 3\mu^2 \left(\frac{m_t^2}{\sin^2 \beta} + \frac{m_b^2}{\cos^2 \beta} \right)^2 + \frac{m_t^2 m_b^2}{\sin^2 \beta \cos^2 \beta} \left(3(A_t + A_b)^2 - \frac{(A_t A_b - \mu^2)^2}{M_{\text{SUSY}}^2} \right) \right]. \quad (61) \end{aligned}$$

5 RG-Improvement and Numerical Results for the MSSM Higgs Masses

The RG-improved Higgs masses (in the absence of squark mixing) are computed by solving the set of coupled REGs for the $\lambda_i(M_{\text{weak}}^2)$, subject to the boundary conditions specified in eq. (33). Squark mixing effects are incorporated into the procedure by modifying the boundary conditions as described in Ref. [37]. Hempfling, Hoang and I [38] found a simple analytic algorithm which reproduces quite accurately the results of the numerical integration of the RGEs.

The procedure starts with the formulae of section 4. The Higgs masses take the form given symbolically in eq. (31). Then,

$$\mathcal{M}_{\text{IRG}}^2 \simeq \overline{\mathcal{M}}_{\text{1LL}}^2 + \Delta \overline{\mathcal{M}}_{\text{mix}}^2 \equiv \mathcal{M}_{\text{1LL}}^2 [m_t(\mu_t), m_b(\mu_b)] + \Delta \mathcal{M}_{\text{mix}}^2 [m_t(\mu_{\bar{t}}), m_b(\mu_{\bar{b}})] , \quad (62)$$

where

$$\mu_t \equiv \sqrt{m_t M_{\text{SUSY}}} , \quad \mu_b \equiv \sqrt{m_b M_{\text{SUSY}}} , \quad \mu_{\bar{q}} \equiv M_{\text{SUSY}} \quad (q = t, b) . \quad (63)$$

That is, the numerically integrated RG-improved CP-even Higgs squared-mass matrix, $\mathcal{M}_{\text{IRG}}^2$, is well approximated by replacing all occurrences of m_t and m_b in $\mathcal{M}_{\text{1LL}}^2(m_t, m_b)$ and $\Delta \mathcal{M}_{\text{mix}}^2(m_t, m_b)$ by the corresponding running masses evaluated at the scales as indicated above.⁶ To implement the above algorithm, we need formulae for $m_b(\mu)$ and $m_t(\mu)$. First, consider $m_{A^0} = \mathcal{O}(m_Z)$. In this case, at mass scales below M_{SUSY} , the effective theory of the Higgs sector is that of a non-supersymmetric two-Higgs-doublet model. In this model, the quark mass is the product of the Higgs-quark Yukawa coupling (h_q) and the appropriate Higgs vacuum expectation value:

$$\begin{aligned} m_b(\mu) &= \frac{1}{\sqrt{2}} h_b(\mu) v_1(\mu) , \\ m_t(\mu) &= \frac{1}{\sqrt{2}} h_t(\mu) v_2(\mu) . \end{aligned} \quad (64)$$

At scales $\mu \leq M_{\text{SUSY}}$, we employ the one-loop non-supersymmetric RGEs of the two-Higgs doublet model for h_b , h_t , and the vacuum expectation values v_1 and v_2 (see Appendix B). This yields

$$\begin{aligned} \frac{d}{d \ln \mu^2} m_b^2 &= \frac{1}{64 \pi^2} \left[6h_b^2 + 2h_t^2 - 32g_s^2 + \frac{4}{3}g'^2 \right] m_b^2 , \\ \frac{d}{d \ln \mu^2} m_t^2 &= \frac{1}{64 \pi^2} \left[6h_t^2 + 2h_b^2 - 32g_s^2 - \frac{8}{3}g'^2 \right] m_t^2 . \end{aligned} \quad (65)$$

⁶In this section, an overline above a quantity will indicate that the replacement of m_t and m_b by the appropriate running mass has been made.

For $m_{A^0} = \mathcal{O}(M_{\text{SUSY}})$, the effective theory of the Higgs sector at mass scales below M_{SUSY} is that of the one-Higgs doublet Standard Model. In this case, we define $m_q(\mu) = h_q^{\text{SM}}(\mu)v(\mu)/\sqrt{2}$, where $v(m_Z) \simeq 246$ GeV is the one-Higgs-doublet Standard Model vacuum expectation value. In this case eq. (65) is modified by replacing $6h_t^2 + 2h_b^2$ with $6(h_t^{\text{SM}})^2 - 6(h_b^{\text{SM}})^2$ in the RGE for m_t^2 (and interchange b and t to obtain the RGE for m_b^2).

To solve these equations, we also need the evolution equations of g_s , and g' . But, an approximate solution is sufficient for our purposes. Since g' is small, we drop it. We do not neglect the h_b dependence which may be significant if $\tan\beta$ is large. Then, we can iteratively solve eq. (65) to one loop by ignoring the μ dependence of the right hand side. We find

$$m_t(\mu) = m_t(m_t) \times \begin{cases} 1 - \frac{1}{\pi} \left[\alpha_s - \frac{1}{16}(\alpha_b + 3\alpha_t) \right] \ln(\mu^2/m_t^2), & m_{A^0} \simeq \mathcal{O}(m_Z), \\ 1 - \frac{1}{\pi} \left[\alpha_s - \frac{3}{16}(\alpha_t^{\text{SM}} - \alpha_b^{\text{SM}}) \right] \ln(\mu^2/m_t^2), & m_{A^0} \simeq \mathcal{O}(M_{\text{SUSY}}), \end{cases} \quad (66)$$

where $\alpha_t \equiv h_t^2/4\pi$, *etc.*, and all coupling on the right hand side are evaluated at m_t . Similarly,

$$m_b(\mu) = m_b(m_Z) \times \begin{cases} 1 - \frac{1}{\pi} \left[\alpha_s - \frac{1}{16}(\alpha_t + 3\alpha_b) \right] \ln(\mu^2/m_Z^2), & m_{A^0} \simeq \mathcal{O}(m_Z), \\ 1 - \frac{1}{\pi} \left[\alpha_s - \frac{3}{16}(\alpha_b^{\text{SM}} - \alpha_t^{\text{SM}}) \right] \ln(\mu^2/m_Z^2), & m_{A^0} \simeq \mathcal{O}(M_{\text{SUSY}}), \end{cases} \quad (67)$$

For intermediate values of m_{A^0} , one may interpolate the above formulae between the two regions. Using eqs. (66) and (67) in eq. (62), and diagonalizing the resulting squared-mass matrix yields our approximation to the RG-improved one-loop neutral CP-even Higgs squared-masses.

We may also apply our algorithm to the radiatively corrected charged Higgs mass. However, in contrast to the one-loop radiatively corrected neutral Higgs mass, there are no one-loop leading logarithmic corrections to $m_{H^\pm}^2$ that are proportional to m_t^4 . Thus, we expect that our charged Higgs mass approximation will not be quite as reliable as our neutral Higgs mass approximation.

Let us now compare various computations of the one-loop corrected light CP-even Higgs mass. In the first set of examples, all squark mixing effects are ignored. First, we evaluate two expressions for the RG-unimproved one-loop Higgs mass—the one-loop leading log Higgs mass calculated from $\mathcal{M}_{\text{1LL}}^2$ and from a simplified version of $\mathcal{M}_{\text{1LL}}^2$ in which only the dominant terms proportional to m_t^4 are kept. In the latter case, we denote the neutral CP-even Higgs squared-mass matrix by $\mathcal{M}_{\text{1LT}}^2 \equiv \mathcal{M}_0^2 + \Delta\mathcal{M}_{\text{1LT}}^2$, where

$$\Delta\mathcal{M}_{\text{1LT}}^2 \equiv \frac{3g^2 m_t^4}{8\pi^2 m_W^2 \sin^2\beta} \ln(M_{\text{SUSY}}^2/m_t^2) \begin{pmatrix} 0 & 0 \\ 0 & 1 \end{pmatrix}. \quad (68)$$

In many analyses of $\mathcal{M}_{\text{ILT}}^2$ and $\mathcal{M}_{\text{ILL}}^2$ that have appeared previously in the literature, the Higgs mass radiative corrections were evaluated with the pole mass, m_t . Some have argued that one should take m_t to be the running mass evaluated at m_t , although to one-loop accuracy, the two choices cannot be distinguished. Nevertheless, because the leading radiative effect is proportional to m_t^4 , the choice of m_t in the one-loop formulae is numerically significant, and can lead to differences as large as 10 GeV in the computed Higgs mass. In Ref. [38], the choice of using $m_t(m_t)$ as opposed to m_t^{pole} (prior to RG-improvement) is justified by invoking information from a two-loop analysis. Thus, our numerical results for the light CP-even Higgs mass before RG-improvement are significantly lower (when M_{SUSY} is large) as compared to the original computations given in the literature, for fixed m_t^{pole} . We have taken $m_t(m_t) = 166.5$ GeV in all the numerical results exhibited below. We then apply our algorithm for RG-improvement by replacing m_t and m_b by the appropriate running masses as specified in eqs. (62)–(63).

We now show examples for $m_{A^0} = 1$ TeV and two choices of $\tan\beta$ in Fig. 1 [$\tan\beta = 20$] and Fig. 2 [$\tan\beta = 1.5$], and for $m_{A^0} = 100$ GeV and $\tan\beta = 20$ in Fig. 3.⁷ Each plot displays five predictions for m_{h^0} based on the following methods for computing the Higgs squared-mass matrix: (i) $\mathcal{M}_{\text{ILT}}^2$; (ii) $\mathcal{M}_{\text{ILL}}^2$; (iii) $\overline{\mathcal{M}}_{\text{ILT}}^2$; (iv) $\overline{\mathcal{M}}_{\text{ILL}}^2$; and (v) $\mathcal{M}_{\text{IRG}}^2$ [the overline notation is defined in the footnote below eq. (63)]. The following general features are noteworthy. First, we observe that over the region of M_{SUSY} shown, $\mathcal{M}_{\text{IRG}}^2 \simeq \overline{\mathcal{M}}_{\text{ILL}}^2$. In fact, m_{h^0} computed from $\overline{\mathcal{M}}_{\text{ILL}}^2$ is within 1 GeV of the numerical RG-improved m_{h^0} in all sensible regions of the parameter space ($1 \leq \tan\beta \leq m_t/m_b$ and $m_t, m_{A^0} \leq M_{\text{SUSY}} \leq 2$ TeV). For values of $M_{\text{SUSY}} > 2$ TeV, the Higgs masses obtained from $\overline{\mathcal{M}}_{\text{ILL}}^2$ begin to deviate from the numerically integrated RG-improved result. Second, the difference between m_{h^0} computed from $\mathcal{M}_{\text{ILL}}^2$ and from $\mathcal{M}_{\text{IRG}}^2$ is non-negligible for large values of M_{SUSY} ; neglecting RG-improvement can lead to an overestimate of m_{h^0} which in some areas of parameter space can be as much as 10 GeV. Finally, note that while the simplest approximation of m_{h^0} based on $\mathcal{M}_{\text{ILT}}^2$ reflects the dominant radiative corrections, it yields the largest overestimate of the light Higgs boson mass.

We next consider some examples in which squark-mixing effects are included. As above, we compare the value of m_{h^0} computed by different procedures. Prior to RG-improvement, we first compute m_{h^0} by diagonalizing $\mathcal{M}_{\text{ILL}}^2 + \Delta\mathcal{M}_{\text{mix}}^2$. Next, we perform RG-improvement as in Ref. [37] by numerically integrating the RGEs for the Higgs self-couplings and inserting the results into eq. (5); the resulting CP-even scalar squared-mass matrix is denoted by $\mathcal{M}_{\text{IRG}}^2$. Finally, we extract m_{h^0} and compare it to the corresponding result obtained by diagonalizing $\overline{\mathcal{M}}_{\text{ILL}}^2 + \Delta\overline{\mathcal{M}}_{\text{mix}}^2$ given by eq. (62). These comparisons are exhibited in a series of figures. First, we plot m_{h^0} vs. X_t/M_{SUSY} for $M_{\text{SUSY}} = m_{A^0} = -\mu = 1$ TeV for two choices of $\tan\beta$

⁷For $m_{A^0} = 100$ GeV and $\tan\beta = 1.5$, the resulting light Higgs mass lies below experimental Higgs mass bounds obtained by the LEP collaborations [14].

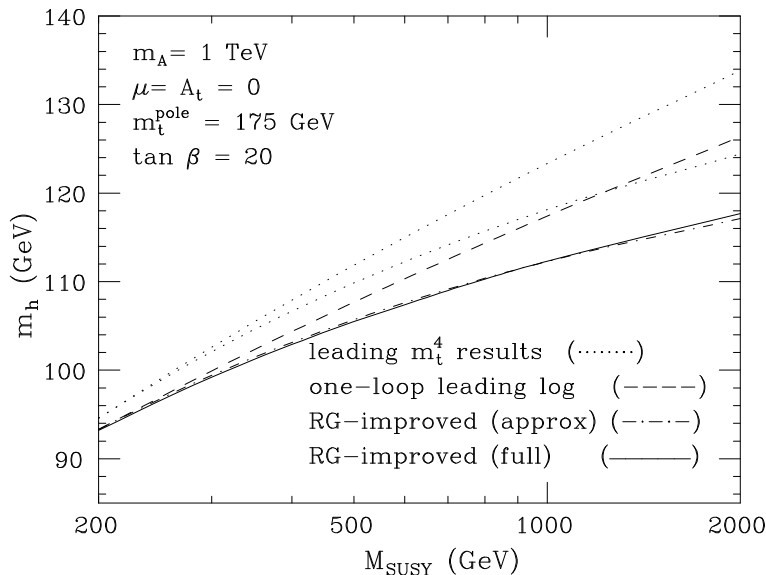


Fig. 1. The radiatively corrected light CP-even Higgs mass is plotted as a function of M_{SUSY} for $\tan \beta = 20$ and $m_{A^0} = 1$ TeV. The one-loop leading logarithmic computation [dashed line] is compared with the RG-improved result which was obtained by numerical analysis [solid line] and by using the simple analytic result given in eq. (62) [dot-dashed line]. For comparison, the results obtained using the leading m_t^4 approximation of eq. (68) [higher dotted line], and its RG-improvement [lower dotted line] are also exhibited. M_{SUSY} characterizes the scale of supersymmetry breaking and can be regarded (approximately) as a common supersymmetric scalar mass; squark mixing effects are set to zero. The running top quark mass used in our numerical computations is $m_t(m_t) = 166.5$ GeV. All figures are taken from Ref. [38].

in Fig. 4 [$\tan \beta = 20$] and Fig. 5 [$\tan \beta = 1.5$]. Note that Fig. 4 is of particular interest, since it allows one to read off the maximal values of m_{h^0} as a function of X_t for $M_{\text{SUSY}} \leq 1$ TeV, which were quoted in section 4.1. The maximum value of the Higgs mass occurs for $|X_t| \simeq 2.4 M_{\text{SUSY}}$.

The reader may worry that this value is too large in light of our perturbative treatment of the squark mixing. However, comparisons with exact diagrammatic computations confirm that these results are trustworthy at least up to the point where the curves reach their maxima. From a more practical point of view, such large values of the mixing are not very natural; they cause tremendous splitting in the top-squark mass eigenstates and are close to the region of parameter space where the $\text{SU}(2) \times \text{U}(1)$ breaking minimum of the scalar potential becomes unstable relative to color and/or electromagnetic breaking vacua [41].

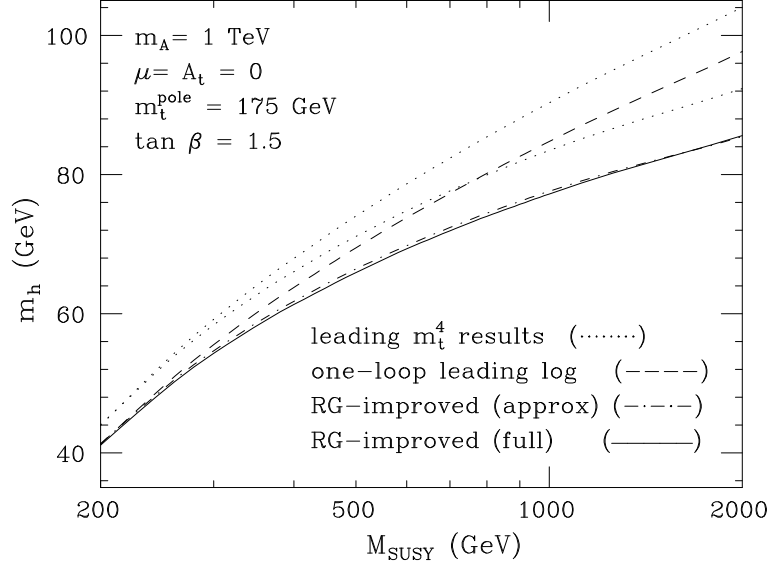


Fig. 2. The radiatively corrected light CP-even Higgs mass is plotted as a function of M_{SUSY} for $\tan \beta = 1.5$ and $m_{A^0} = 1 \text{ TeV}$. See the caption to Fig. 1.

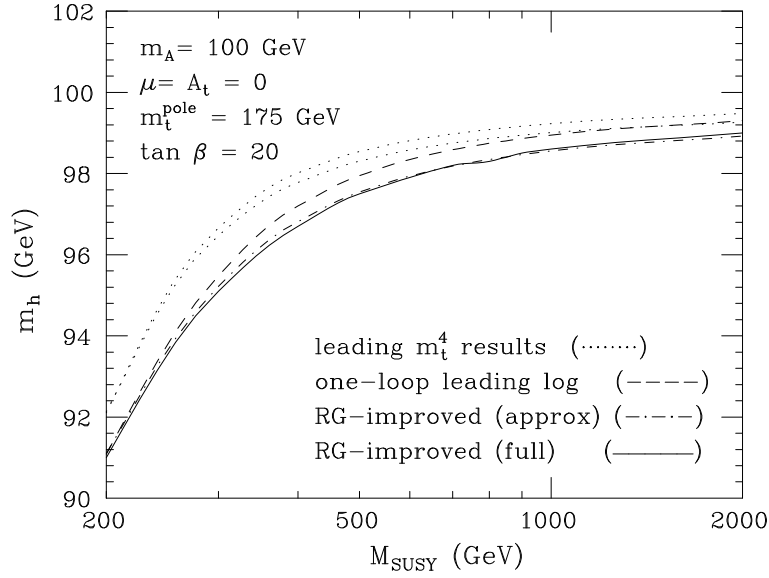


Fig. 3. The radiatively corrected light CP-even Higgs mass is plotted as a function of M_{SUSY} for $\tan \beta = 20$ and $m_{A^0} = 100 \text{ GeV}$. See the caption to Fig. 1.

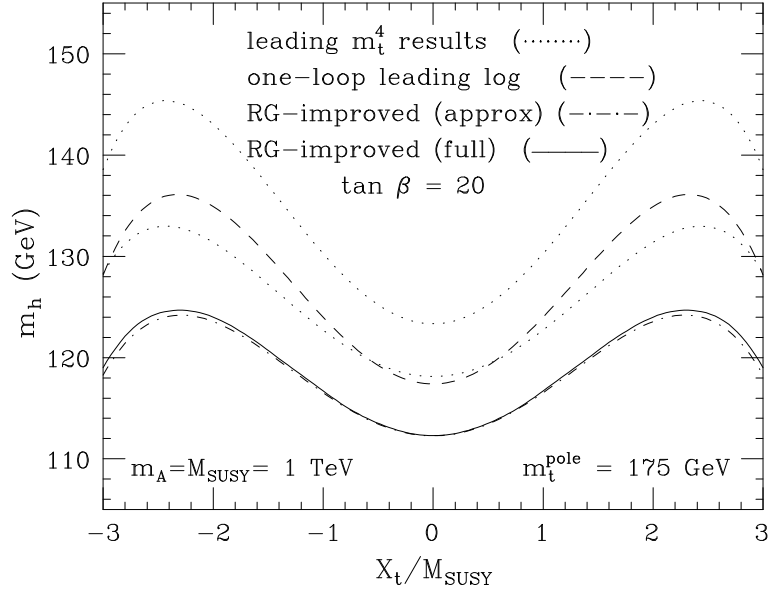


Fig. 4. The radiatively corrected light CP-even Higgs mass is plotted as a function of X_t/M_{SUSY} , where $X_t \equiv A_t - \mu \cot \beta$, for $M_{\text{SUSY}} = m_{A^0} = -\mu = 1 \text{ TeV}$ and $\tan \beta = 20$. See the caption to Fig. 1.

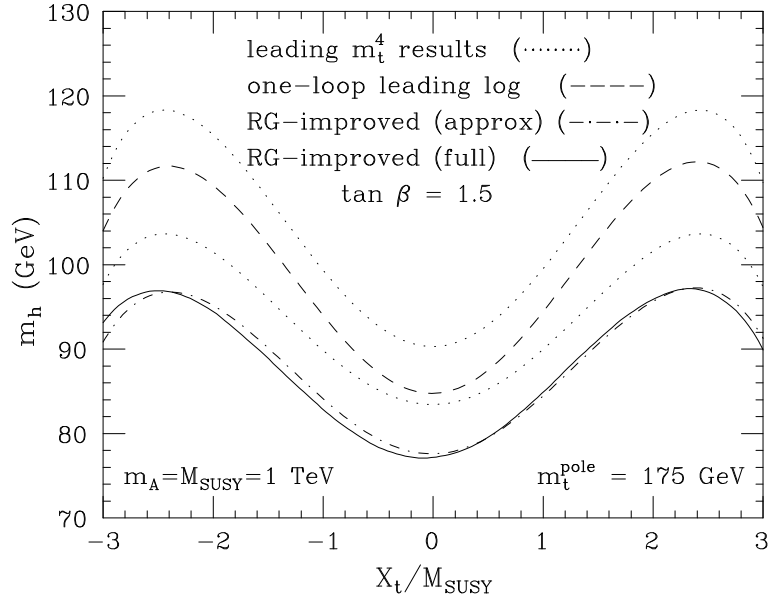


Fig. 5. The radiatively corrected light CP-even Higgs mass is plotted as a function of X_t/M_{SUSY} , where $X_t \equiv A_t - \mu \cot \beta$, for $M_{\text{SUSY}} = m_{A^0} = -\mu = 1 \text{ TeV}$ and $\tan \beta = 1.5$. See the caption to Fig. 1.

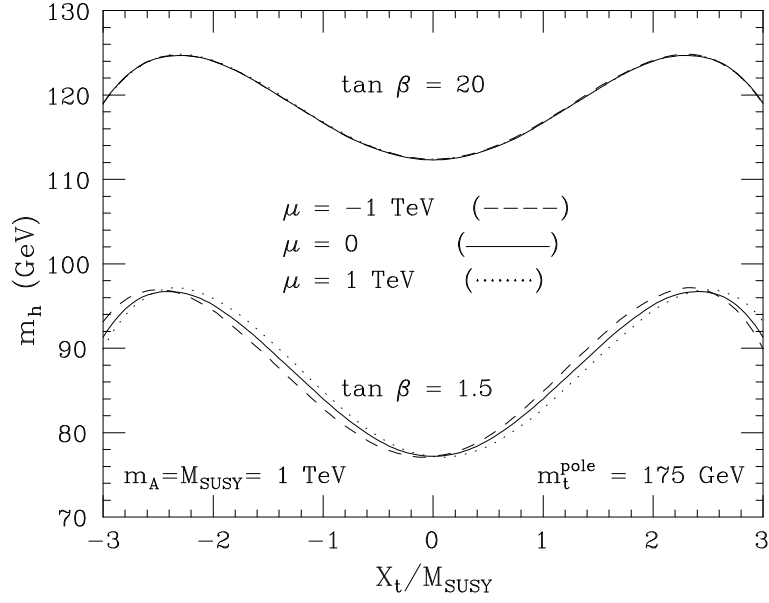


Fig. 6. The radiatively corrected, RG-improved light CP-even Higgs mass is plotted as a function of X_t/M_{SUSY} , where $X_t \equiv A_t - \mu \cot \beta$, for $M_{\text{SUSY}} = m_{A^0} = 1$ TeV and two choices of $\tan \beta = 1.5$ and 20 . Three values of μ are plotted in each case: -1 TeV [dashed], 0 [solid] and 1 TeV [dotted]. Here, we have assumed that the diagonal squark squared-masses are degenerate: $M_Q = M_U = M_D = M_{\text{SUSY}}$.

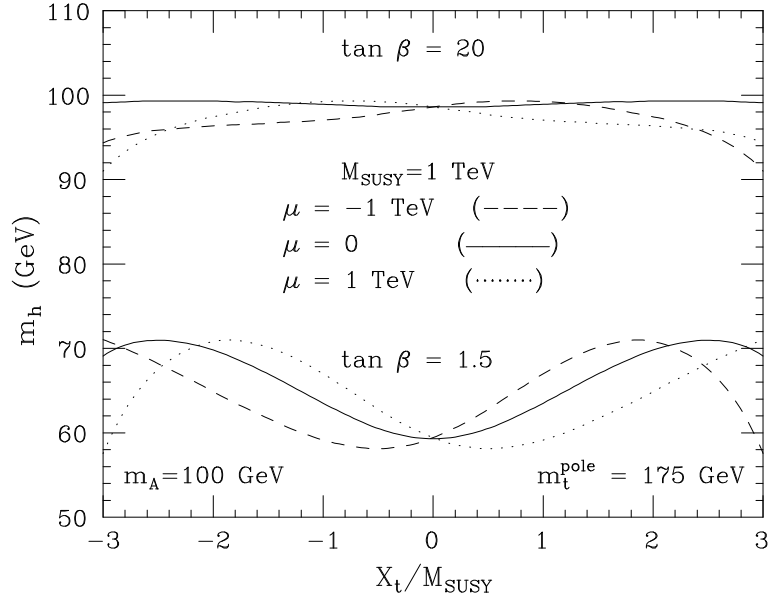


Fig. 7. The radiatively corrected, RG-improved light CP-even Higgs mass is plotted as a function of X_t/M_{SUSY} for $M_{\text{SUSY}} = 1$ TeV and $m_{A^0} = 100$ GeV. See the caption to Fig. 6.

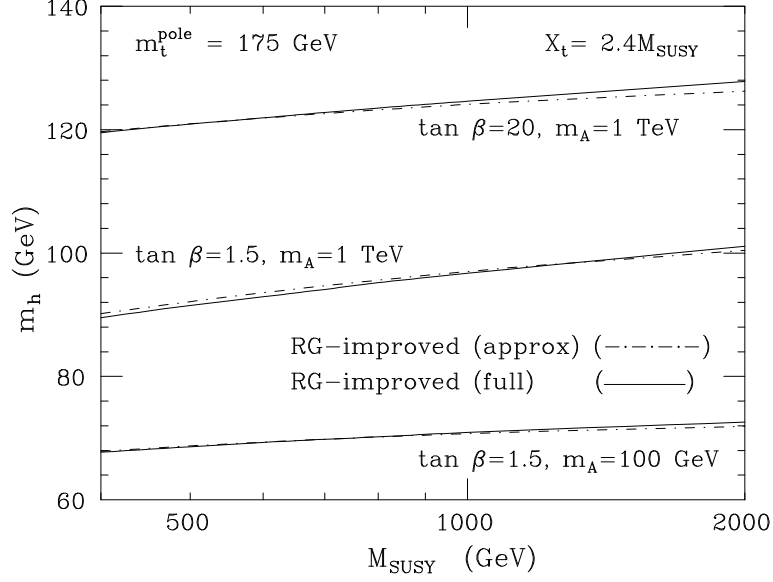


Fig. 8. The radiatively corrected, RG-improved light CP-even Higgs mass is plotted as a function of M_{SUSY} for $X_t = 2.4 M_{\text{SUSY}}$ for three choices of $(\tan \beta, m_{A^0}) = (20, 1)$, $(1.5, 1)$, and $(1.5, 0.1)$, where m_{A^0} is specified in TeV units. The solid line depicts the numerically integrated result, and the dot-dashed line indicates the result obtained from eq. (62).

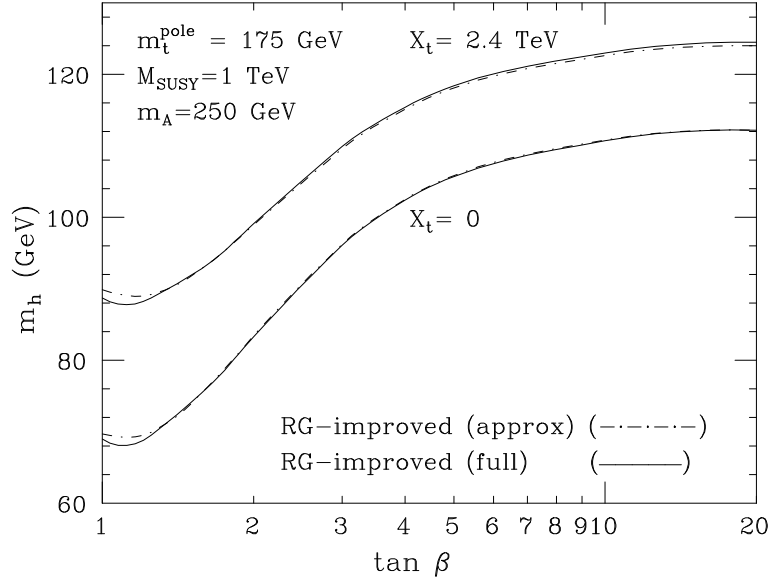


Fig. 9. The radiatively corrected, RG-improved light CP-even Higgs mass is plotted as a function of $\tan \beta$ for $M_{\text{SUSY}} = 1$ TeV and $m_{A^0} = 250$ GeV, for two choices of $X_t = 0$ and $X_t = 2.4 M_{\text{SUSY}}$. See the caption to Fig. 8.

In Figs. 4 and 5, $\mu = -1$ TeV, *i.e.*, as $X_t \equiv A_t - \mu \cot \beta$ varies, so does A_t . In fact, for $m_{A^0} \gg m_Z$, the dominant one-loop radiative corrections to $m_{h^0}^2$ depend only on X_t and M_{SUSY} [see eq. (60)], so that for fixed X_t , the μ dependence of m_{h^0} is quite weak. This is illustrated in Fig. 6. For values of $m_{A^0} \sim \mathcal{O}(m_Z)$, the μ dependence is slightly more pronounced (although less so for values of $\tan \beta \gg 1$) as illustrated in Fig. 7. We also display m_{h^0} as a function of M_{SUSY} for a number of different parameter choices in Fig. 8. In Fig. 9, we exhibit the $\tan \beta$ dependence of m_{h^0} for two different choices of X_t . Again, we notice that our approximate formula [eq. (62)], which is depicted by the dot-dashed line, does remarkably well, and never differs from the numerically integrated RG-improved value (solid line) by more than 1.5 GeV for $M_{\text{SUSY}} \leq 2$ TeV and $\tan \beta \geq 1$.

In summary, when the algorithm given by eqs. (62) and (63) is applied to the leading log one-loop corrections plus the leading terms resulting from squark mixing, the full (numerically integrated) RG-improved value of m_{h^0} is reproduced to within an accuracy of about 2 GeV (assuming that supersymmetric particle masses lie below 2 TeV). The methods described above also yield accurate results for the mass of the heavier CP-even Higgs boson, m_{H^0} . The approximation to the radiatively corrected charged Higgs mass is slightly less accurate only because the leading m_t enhanced terms are not as dominant as in the neutral Higgs sector.⁸

6 Implications of the Radiatively Corrected Higgs Sector

Using the results of sections 4 and 5, one can obtain the leading radiative corrections to the various Higgs couplings, and proceed to investigate Higgs phenomenology in detail. Here, I shall describe the procedure used to obtain the Higgs couplings and briefly indicate some of the consequences. To obtain radiatively corrected couplings which are accurate in the one-loop leading logarithmic approximation, it is sufficient to use the tree-level couplings in which the parameters are taken to be running parameters evaluated at the electroweak scale. First, I remind the reader that $\tan \beta$ and m_{A^0} are input parameters. Next, we obtain the CP-even Higgs mixing angle α by diagonalizing the radiatively corrected CP-even Higgs mass matrix. With the angle α in hand one may compute, for example, $\cos(\beta - \alpha)$ and $\sin \alpha$. These results can be used to obtain the Higgs couplings to gauge bosons [eq. (14)] and fermions [eq. (15)]. Finally, the Higgs self-couplings [see Appendix A] are obtained by making use of the λ_i evaluated at the electroweak scale. The end result is a complete set of Higgs boson decay widths and branching ratios that include one-loop leading-log radiative corrections.

⁸The approximation to the radiatively corrected charged Higgs mass can be improved by including sub-dominant terms not contained in the formulae given in this paper; see Ref. [31] for further details.

The Higgs production cross-section in a two-Higgs-doublet model via the process $e^+e^- \rightarrow Z \rightarrow ZH^0(Zh^0)$ is suppressed by a factor $\cos^2(\beta - \alpha)$ [$\sin^2(\beta - \alpha)$] as compared to the corresponding cross-sections in the Standard Model. At tree-level, we know that the decoupling limit applies when $m_{A^0} \gg m_Z$. In fact, the approach to decoupling is quite rapid as indicated in eq. (28). For $m_{A^0} \gtrsim 2m_Z$, the couplings of h^0 to vector bosons and to quarks and leptons are phenomenologically indistinguishable from those of the Standard Model Higgs boson. Including radiative corrections does not alter this basic behavior, although one finds that $\cos^2(\beta - \alpha) \rightarrow 0$ more slowly as the radiative corrections become more significant.

When radiative corrections have been incorporated, new possibilities arise which did not exist at tree-level. One example is the possibility of the decay $h^0 \rightarrow A^0 A^0$, which is kinematically forbidden at tree-level but is allowed for some range of MSSM parameters [26,42]. We can obtain the complete one-loop leading-log expression for the $h^0 A^0 A^0$ coupling (assuming $m_{A^0} \lesssim m_Z$) by inserting the one-loop leading-log formulae for the λ_i into eq. (A.1) [42]

$$\begin{aligned} \frac{g_{h^0 A^0 A^0}}{gm_Z/2c_W} = & -c_{2\beta}s_{\beta+\alpha} \left\{ 1 + \frac{g^2}{96\pi^2 c_W^2} \left[P_t \ln\left(\frac{M_{\text{SUSY}}^2}{m_t^2}\right) + (P_b + P_f) \ln\left(\frac{M_{\text{SUSY}}^2}{m_Z^2}\right) \right] \right\} \\ & + \frac{g^2 N_c}{16\pi^2 m_W^2 m_Z^2} \left\{ \left[\frac{s_\alpha s_\beta^2}{c_\beta^3} (2m_b^4 - m_b^2 m_Z^2 c_\beta^2) - \frac{(c_\alpha s_\beta^3 - s_\alpha c_\beta^3)}{2c_\beta^2} m_b^2 m_Z^2 \right] \ln\left(\frac{M_{\text{SUSY}}^2}{m_Z^2}\right) \right. \\ & - \left[\frac{c_\alpha c_\beta^2}{s_\beta^3} (2m_t^4 - m_t^2 m_Z^2 s_\beta^2) + \frac{(c_\alpha s_\beta^3 - s_\alpha c_\beta^3)}{2s_\beta^2} m_t^2 m_Z^2 \right] \ln\left(\frac{M_{\text{SUSY}}^2}{m_t^2}\right) \left. \right\} \\ & - \frac{g^2}{192\pi^2 c_W^2} \left[s_{2\beta} c_{\beta+\alpha} (P_{2H} + P_g) - 2(c_\alpha s_\beta^3 - s_\alpha c_\beta^3) (P'_{2H} + P'_g) \right] \ln\left(\frac{M_{\text{SUSY}}^2}{m_Z^2}\right). \end{aligned} \quad (69)$$

If kinematically allowed, $h^0 \rightarrow A^0 A^0$ would almost certainly be the dominant decay mode. However, the LEP experimental lower bound on m_{A^0} now lies above $0.5(m_{h^0})_{\text{max}} \simeq 62.5$ GeV. Thus, the region of parameter space where the decay $h^0 \rightarrow A^0 A^0$ is kinematically allowed is no longer viable. The possibility of measuring the $h^0 A^0 A^0$ couplings at a future e^+e^- linear collider by detecting double Higgs production has been discussed in Ref. [43]. Unfortunately, the prospects are poor due to low cross-sections and significant backgrounds.

For the heavier Higgs states, there are many possible final state decay modes. The various branching ratios are complicated functions of the MSSM parameter space [44]. For example, a plot of the branching ratios of H^0 , with the leading one-loop radiative corrections included, can be found in Ref. [45]. This plot indicates a rich phenomenology for heavy Higgs searches at future colliders. The precision

measurements of Higgs masses and couplings will be one of the primary tasks of the LHC and future lepton-lepton colliders [46,47]

Although the possibility of a light Higgs discovery at LEP still remains, the effects of the radiative corrections may be significant enough to push the Higgs boson above the LEP-2 discovery reach. In this case, the discovery of the Higgs boson will be the purview of the LHC. Of course, if low-energy supersymmetry exists, then LHC will also uncover direct evidence for the supersymmetric particles. In this case, a detailed examination of the Higgs sector, with precision measurements of the Higgs masses and couplings, will provide a critical test for the underlying supersymmetric structure. Unlocking the secrets of the Higgs bosons will help reveal the mechanism of electroweak symmetry breaking and the nature of the TeV scale physics that lies beyond the Standard Model.

Acknowledgments

I would like to express my deep appreciation to my collaborators Ralf Hempfling and Andre Hoang, whose contributions to the work on radiatively corrected Higgs masses were instrumental to the development of the material reported in this paper. I would also like to thank Marco Díaz, Abdel Djouadi, Yuval Grossman, Jack Gunion, Yossi Nir, Scott Thomas, and Peter Zerwas for many fruitful interactions. Finally, I gratefully acknowledge conversations with Marcela Carena, Mariano Quiros and Carlos Wagner and appreciate the opportunity provided by the 1995 LEP-2 workshop to revisit many of the issues discussed here. This work was supported in part by the U.S. Department of Energy.

Appendix

A Three-Higgs Vertices in the Two-Higgs Doublet Model

In this Appendix, I list the Feynman rules for the 3-point Higgs interaction in the most general (nonsupersymmetric) two-Higgs doublet extension of the Standard Model, assuming that the Higgs sector conserves CP. The Feynman rule for the ABC vertex is denoted by ig_{ABC} . For completeness, R -gauge Feynman rules involving the Goldstone bosons (G^\pm and G^0) are also listed.

Interactions involving physical Higgs bosons depend in detail on the parameters of the Higgs potential specified in eq. (1).

$$\begin{aligned}
g_{h^0 A^0 A^0} &= \frac{2m_W}{g} \left[\lambda_1 s_\beta^2 c_\beta s_\alpha - \lambda_2 c_\beta^2 s_\beta c_\alpha - \tilde{\lambda}_3 (s_\beta^3 c_\alpha - c_\beta^3 s_\alpha) + 2\lambda_5 s_{\beta-\alpha} \right. \\
&\quad \left. - \lambda_6 s_\beta (c_\beta s_{\alpha+\beta} + s_\alpha c_{2\beta}) - \lambda_7 c_\beta (c_\alpha c_{2\beta} - s_\beta s_{\alpha+\beta}) \right], \\
g_{H^0 A^0 A^0} &= \frac{-2m_W}{g} \left[\lambda_1 s_\beta^2 c_\beta c_\alpha + \lambda_2 c_\beta^2 s_\beta s_\alpha + \tilde{\lambda}_3 (s_\beta^3 s_\alpha + c_\beta^3 c_\alpha) - 2\lambda_5 c_{\beta-\alpha} \right. \\
&\quad \left. - \lambda_6 s_\beta (c_\beta c_{\alpha+\beta} + c_\alpha c_{2\beta}) + \lambda_7 c_\beta (s_\beta c_{\alpha+\beta} + s_\alpha c_{2\beta}) \right], \\
g_{h^0 H^0 H^0} &= \frac{6m_W}{g} \left[\lambda_1 c_\alpha^2 c_\beta s_\alpha - \lambda_2 s_\alpha^2 s_\beta c_\alpha + \tilde{\lambda}_3 (s_\alpha^3 c_\beta - c_\alpha^3 s_\beta + \frac{2}{3} s_{\beta-\alpha}) \right. \\
&\quad \left. - \lambda_6 c_\alpha (c_\beta c_{2\alpha} - s_\alpha s_{\alpha+\beta}) - \lambda_7 c_\alpha (s_\beta c_{2\alpha} + c_\alpha s_{\alpha+\beta}) \right], \\
g_{H^0 h^0 h^0} &= \frac{-6m_W}{g} \left[\lambda_1 s_\alpha^2 c_\beta c_\alpha + \lambda_2 c_\alpha^2 s_\beta s_\alpha + \tilde{\lambda}_3 (s_\alpha^3 s_\beta + c_\alpha^3 c_\beta - \frac{2}{3} c_{\beta-\alpha}) \right. \\
&\quad \left. - \lambda_6 s_\alpha (c_\beta c_{2\alpha} + c_\alpha c_{\alpha+\beta}) + \lambda_7 c_\alpha (s_\beta c_{2\alpha} + s_\alpha c_{\alpha+\beta}) \right], \\
g_{h^0 h^0 h^0} &= \frac{6m_W}{g} \left[\lambda_1 s_\alpha^3 c_\beta - \lambda_2 c_\alpha^3 s_\beta + \tilde{\lambda}_3 s_\alpha c_\alpha c_{\alpha+\beta} \right. \\
&\quad \left. - \lambda_6 s_\alpha^2 (3c_\alpha c_\beta - s_\alpha s_\beta) + \lambda_7 c_\alpha^2 (3s_\alpha s_\beta - c_\alpha c_\beta) \right], \\
g_{H^0 H^0 H^0} &= \frac{-6m_W}{g} \left[\lambda_1 c_\alpha^3 c_\beta + \lambda_2 s_\alpha^3 s_\beta + \tilde{\lambda}_3 s_\alpha c_\alpha s_{\alpha+\beta} \right. \\
&\quad \left. + \lambda_6 c_\alpha^2 (3s_\alpha c_\beta + c_\alpha s_\beta) + \lambda_7 s_\alpha^2 (3c_\alpha s_\beta + s_\alpha c_\beta) \right], \\
g_{h^0 H^+ H^-} &= g_{h^0 A^0 A^0} - \frac{2m_W}{g} (\lambda_5 - \lambda_4) s_{\beta-\alpha}, \\
g_{H^0 H^+ H^-} &= g_{H^0 A^0 A^0} - \frac{2m_W}{g} (\lambda_5 - \lambda_4) c_{\beta-\alpha},
\end{aligned} \tag{A.1}$$

where I have used the notation

$$\tilde{\lambda}_3 \equiv \lambda_3 + \lambda_4 + \lambda_5. \quad (\text{A.2})$$

It is interesting to note that couplings of the charged Higgs bosons satisfy relations analogous to that of m_{H^\pm} given in eq. (4).

The Feynman rules for three-point Higgs vertices that involve Goldstone bosons exhibit much simpler forms

$$\begin{aligned} g_{h^0 G^0 G^0} &= \frac{-g}{2m_W} m_{h^0}^2 \sin(\beta - \alpha), \\ g_{H^0 G^0 G^0} &= \frac{-g}{2m_W} m_{H^0}^2 \cos(\beta - \alpha), \\ g_{h^0 G^+ G^-} &= g_{h^0 G^0 G^0}, \\ g_{H^0 G^+ G^-} &= g_{H^0 G^0 G^0}, \\ g_{h^0 A^0 G^0} &= \frac{-g}{2m_W} (m_{h^0}^2 - m_{A^0}^2) \cos(\beta - \alpha), \\ g_{H^0 A^0 G^0} &= \frac{g}{2m_W} (m_{H^0}^2 - m_{A^0}^2) \sin(\beta - \alpha), \\ g_{h^0 H^\pm G^\mp} &= \frac{g}{2m_W} (m_{H^\pm}^2 - m_{h^0}^2) \cos(\beta - \alpha), \\ g_{H^0 H^\pm G^\mp} &= \frac{-g}{2m_W} (m_{H^\pm}^2 - m_{H^0}^2) \sin(\beta - \alpha), \\ g_{A^0 H^\pm G^\mp} &= \frac{\pm g}{2m_W} (m_{H^\pm}^2 - m_{A^0}^2). \end{aligned} \quad (\text{A.3})$$

In the rule for the $A^0 H^\pm G^\mp$ vertex, the sign corresponds to H^\pm entering the vertex and G^\pm leaving the vertex.

One can easily check that if tree-level MSSM relations are imposed on the λ_i , Higgs masses, and angles α and β , one recovers the MSSM Feynman rules listed in Appendix A of Ref. [1].

B Renormalization Group Equations

In this Appendix, I have collected the one-loop renormalization group equations (RGEs) that are needed in the analysis presented in this paper [39,48,37]. Schematically, the RGEs at one-loop take the form

$$\frac{dp_i}{dt} = \beta_i(p_1, p_2, \dots), \quad \text{where } t \equiv \ln \mu^2, \quad (\text{B.1})$$

where μ is the energy scale, and the parameters p_i stand for the Higgs boson self-couplings λ_i ($i = 1 \dots 7$), the squared Yukawa couplings h_f^2 ($f = t, b$ and τ ; the two lighter generations can be neglected), and the squared gauge couplings g_j^2 ($j = 3, 2, 1$) corresponding to $\text{SU}(3) \times \text{SU}(2) \times \text{U}(1)$ respectively. The g_j are normalized such that they are equal at the grand unification scale. It is also convenient to define

$$g \equiv g_2, \quad g' \equiv \sqrt{\frac{3}{5}} g_1, \quad (\text{B.2})$$

where g and g' are normalized in the usual way for low-energy electroweak physics, *i.e.* $\tan \theta_W = g'/g$.

I now list the β -functions required for the analysis presented in this paper. Two cases will be given, depending on whether μ is above or below the scale of supersymmetry breaking, M_{SUSY} .

1. $\mu > M_{\text{SUSY}}$

$$\begin{aligned} \beta_{h_t^2} &= \frac{h_t^2}{16\pi^2} \left[6h_t^2 + h_b^2 - \frac{16}{3}g_3^2 - 3g^2 - \frac{13}{9}g'^2 \right] \\ \beta_{h_b^2} &= \frac{h_b^2}{16\pi^2} \left[6h_b^2 + h_t^2 + h_\tau^2 - \frac{16}{3}g_3^2 - 3g^2 - \frac{7}{9}g'^2 \right] \\ \beta_{h_\tau^2} &= \frac{h_\tau^2}{16\pi^2} \left[4h_\tau^2 + 3h_b^2 - 3g^2 - 3g'^2 \right] \\ \beta_{g'^2} &= \frac{g'^4}{48\pi^2} \left[10N_g + \frac{3}{2}N_H \right] \\ \beta_{g^2} &= \frac{g^4}{48\pi^2} \left[6N_g + \frac{3}{2}N_H - 18 \right] \\ \beta_{g_3^2} &= \frac{g_3^4}{48\pi^2} \left[6N_g - 27 \right]. \end{aligned} \quad (\text{B.3})$$

Here $N_g = 3$ is the number of generations, $N_H = 2$ is the number of scalar doublets, and the Higgs-fermion Yukawa couplings are given by

$$\begin{aligned}
h_t &= \frac{gm_t}{\sqrt{2}m_W \sin \beta}, \\
h_{d_i} &= \frac{gm_{d_i}}{\sqrt{2}m_W \cos \beta}, \quad (d_i = b, \tau).
\end{aligned} \tag{B.4}$$

2. $\mu < M_{\text{SUSY}}$

$$\begin{aligned}
\beta_{h_t^2} &= \frac{h_t^2}{16\pi^2} \left[\frac{9}{2}h_t^2 + \frac{1}{2}h_b^2 - 8g_3^2 - \frac{9}{4}g^2 - \frac{17}{12}g'^2 \right] \\
\beta_{h_b^2} &= \frac{h_b^2}{16\pi^2} \left[\frac{9}{2}h_b^2 + \frac{1}{2}h_t^2 + h_\tau^2 - 8g_3^2 - \frac{9}{4}g^2 - \frac{5}{12}g'^2 \right] \\
\beta_{h_\tau^2} &= \frac{h_\tau^2}{16\pi^2} \left[\frac{5}{2}h_\tau^2 + 3h_b^2 - \frac{9}{4}g^2 - \frac{15}{4}g'^2 \right] \\
\beta_{g'^2} &= \frac{g'^4}{48\pi^2} \left[\frac{20}{3}N_g + \frac{1}{2}N_H \right] \\
\beta_{g^2} &= \frac{g^4}{48\pi^2} \left[4N_g + \frac{1}{2}N_H - 22 \right] \\
\beta_{g_3^2} &= \frac{g_3^4}{48\pi^2} \left[4N_g - 33 \right].
\end{aligned} \tag{B.5}$$

In writing down the RGEs for the Higgs-fermion Yukawa couplings in eq. (B.5), I have assumed that the Higgs-fermion interaction is the same as in the MSSM; namely, Φ_1 [Φ_2] couples exclusively to down-type [up-type] fermions. Moreover, in deriving the $\mu < M_{\text{SUSY}}$ equations, it was assumed that the effective low-energy theory at the scale μ includes the full two-doublet Higgs sector (but does not include the supersymmetric particles, whose masses are of order M_{SUSY}).

Finally, I list the RGEs for the Higgs self-couplings of the general two-Higgs doublet model (with the Higgs-fermion couplings as specified above). First, I need to define the anomalous dimensions of the two Higgs fields:

$$\begin{aligned}
\gamma_1 &= \frac{1}{64\pi^2} \left[9g^2 + 3g'^2 - 4 \sum_i N_{ci} h_{d_i}^2 \right], \\
\gamma_2 &= \frac{1}{64\pi^2} \left[9g^2 + 3g'^2 - 4 \sum_i N_{ci} h_{u_i}^2 \right],
\end{aligned} \tag{B.6}$$

where the sum over i is taken over three generations of quarks (with $N_c = 3$) and leptons (with $N_c = 1$). The β -functions for the Higgs self-couplings in the general CP-conserving non-supersymmetric two-Higgs-doublet model (with the Higgs-fermion couplings as specified in section 2) are given by

$$\begin{aligned}
\beta_{\lambda_1} &= \frac{1}{16\pi^2} \left\{ 6\lambda_1^2 + 2\lambda_3^2 + 2\lambda_3\lambda_4 + \lambda_4^2 + \lambda_5^2 + 12\lambda_6^2 \right. \\
&\quad \left. + \frac{3}{8} [2g^4 + (g^2 + g'^2)^2] - 2 \sum_i N_{ci} h_{di}^4 \right\} - 2\lambda_1\gamma_1 \\
\beta_{\lambda_2} &= \frac{1}{16\pi^2} \left\{ 6\lambda_2^2 + 2\lambda_3^2 + 2\lambda_3\lambda_4 + \lambda_4^2 + \lambda_5^2 + 12\lambda_7^2 \right. \\
&\quad \left. + \frac{3}{8} [2g^4 + (g^2 + g'^2)^2] - 2 \sum_i N_{ci} h_{ui}^4 \right\} - 2\lambda_2\gamma_2 \\
\beta_{\lambda_3} &= \frac{1}{16\pi^2} \left\{ (\lambda_1 + \lambda_2)(3\lambda_3 + \lambda_4) + 2\lambda_3^2 + \lambda_4^2 + \lambda_5^2 + 2\lambda_6^2 + 2\lambda_7^2 + 8\lambda_6\lambda_7 \right. \\
&\quad \left. + \frac{3}{8} [2g^4 + (g^2 - g'^2)^2] - 2 \sum_i N_{ci} h_{ui}^2 h_{di}^2 \right\} - \lambda_3(\gamma_1 + \gamma_2) \\
\beta_{\lambda_4} &= \frac{1}{16\pi^2} \left[\lambda_4(\lambda_1 + \lambda_2 + 4\lambda_3 + 2\lambda_4) + 4\lambda_5^2 + 5\lambda_6^2 + 5\lambda_7^2 + 2\lambda_6\lambda_7 \right. \\
&\quad \left. + \frac{3}{2} g^2 g'^2 + 2 \sum_i N_{ci} h_{ui}^2 h_{di}^2 \right] - \lambda_4(\gamma_1 + \gamma_2) \\
\beta_{\lambda_5} &= \frac{1}{16\pi^2} \left[\lambda_5(\lambda_1 + \lambda_2 + 4\lambda_3 + 6\lambda_4) + 5(\lambda_6^2 + \lambda_7^2) + 2\lambda_6\lambda_7 \right] - \lambda_5(\gamma_1 + \gamma_2) \\
\beta_{\lambda_6} &= \frac{1}{16\pi^2} \left[\lambda_6(6\lambda_1 + 3\lambda_3 + 4\lambda_4 + 5\lambda_5) + \lambda_7(3\lambda_3 + 2\lambda_4 + \lambda_5) \right] - \frac{1}{2}\lambda_6(3\gamma_1 + \gamma_2) \\
\beta_{\lambda_7} &= \frac{1}{16\pi^2} \left[\lambda_7(6\lambda_2 + 3\lambda_3 + 4\lambda_4 + 5\lambda_5) + \lambda_6(3\lambda_3 + 2\lambda_4 + \lambda_5) \right] - \frac{1}{2}\lambda_7(\gamma_1 + 3\gamma_2).
\end{aligned}
\tag{B.7}$$

References

- [1] J.F. Gunion, H.E. Haber, G. Kane and S. Dawson, *The Higgs Hunter's Guide* (Addison-Wesley Publishing Company, Reading, MA, 1990).
- [2] H.E. Haber, in *Testing the Standard Model*, Proceedings of the 1990 Theoretical Advanced Study Institute in Elementary Particle Physics, edited by M. Cvetič and P. Langacker (World Scientific, Singapore, 1991) p. 340–475.
- [3] G. 't Hooft, in *Recent Developments in Gauge Theories*, Proceedings of the NATO Advanced Summer Institute, Cargèse, 1979, edited by G. 't Hooft *et al.* (Plenum, New York, 1980) p. 135–157.
- [4] L. Susskind, *Phys. Rep.* **104** (1984) 181.
- [5] E. Witten, *Nucl. Phys.* **B188** (1981) 513; S. Dimopoulos and H. Georgi, *Nucl. Phys.* **B193** (1981) 150; N. Sakai, *Z. Phys.* **C11** (1981) 153; R.K. Kaul, *Phys. Lett.* **109B** (1982) 19.
- [6] H.P. Nilles, *Phys. Rep.* **110** (1984) 1; H.E. Haber and G.L. Kane, *Phys. Rep.* **117** (1985) 75; A.B. Lahanas and D.V. Nanopoulos, *Phys. Rep.* **145** (1987) 1; R. Barbieri, *Riv. Nuovo Cimento* **11** (1988) 1; R. Arnowitt and P. Nath, in *Particles and Fields*, Proceedings of the VII Jorge Andre Swieca Summer School, Sao Paulo, Brazil, 10–23 January, 1993, edited by J.P. Eboli and V.O. Rivelles (World Scientific, Singapore, 1994) pp. 3–63.
- [7] H.E. Haber, *Phys. Rev.* **D54** (1996) 687; H.E. Haber, in *Recent Directions in Particle Theory*, Proceedings of the 1992 Theoretical Advanced Study Institute in Elementary Particle Physics, edited by J. Harvey and J. Polchinski (World Scientific, Singapore, 1993) pp. 589–686.
- [8] For a comprehensive review and a guide to the literature, see Chapter 4 of Ref. [1].
- [9] J.M. Cornwall, D.N. Levin and G. Tiktopoulos, *Phys. Rev. Lett.* **30** (1973) 1268; *Phys. Rev.* **D10** (1974) 1145; C.H. Llewellyn Smith, *Phys. Lett.* **46B** (1973) 233; H.A. Weldon, *Phys. Rev.* **D30** (1984) 1547; J.F. Gunion, H.E. Haber and J. Wudka, *Phys. Rev.* **D43** (1991) 904.
- [10] J.F. Gunion and H.E. Haber, *Nucl. Phys.* **B272** (1986) 1; **B278** (1986) 449 [E: **B402** (1993) 567].
- [11] S. Glashow and S. Weinberg, *Phys. Rev.* **D15** (1977) 1958; E.A. Paschos, *Phys. Rev.* **D15** (1977) 1966.

- [12] H. E. Haber and Y. Nir, *Nucl. Phys.* **B335** (1990) 363.
- [13] H.E. Haber, in *Beyond the Standard Model IV*, Proceedings of the Fourth International Conference on Physics Beyond the Standard Model, Granlibakken, Lake Tahoe, CA, 13–18 December, 1994, edited by J.F. Gunion, T. Han and J. Ohnemus (World Scientific, Singapore, 1995) pp. 151–163; and in *Perspectives for Electroweak Interactions in e^+e^- Collisions*, Proceedings of the Ringberg Workshop, Ringberg Castle, Tegernsee, Germany, 5–8 February, 1995, edited by B.A. Kniehl (World Scientific, Singapore, 1995) pp. 219–231.
- [14] J.P. Martin, LYCEN-9644 (1996), in Proceedings of the 28th International Conference on High Energy Physics, Warsaw, Poland, 25–31 July 1996, edited by Z. Ajduk and A.K. Wroblewski (World Scientific, Singapore, 1997).
- [15] M. Carena, P.M. Zerwas *et al.*, in *Physics at LEP2*, Volume 1, edited by G. Altarelli, T. Sjöstrand and F. Zwirner, CERN Yellow Report 96-01 (1996) pp. 351–462.
- [16] R. Barate *et al.* [ALEPH Collaboration], CERN-PPE/97-70 (1997); CERN-PPE/97-71 (1997), submitted to *Phys. Lett. B*.
- [17] A.K. Grant, *Phys. Rev.* **D51** (1995) 207.
- [18] J.L. Hewett, *Phys. Rev. Lett.* **70** (1993) 1045; V. Barger, M. Berger and R.J.N. Phillips, *Phys. Rev. Lett.* **70** (1993) 1368; J.L. Hewett, in *B Physics: Physics Beyond the Standard Model at the B Factory*, Proceedings of the International Workshop on B Physics, Nagoya, Japan, 26–28 October 1994, edited by A.I. Sanda and S. Suzuki (World Scientific, Singapore, 1995) pp. 321–326.
- [19] Y. Grossman, H.E. Haber and Y. Nir, *Phys. Lett.* **B357** (1995) 630.
- [20] J.A. Coarasa, R.A. Jiménez and J. Solà, UAB-FT-407 (1997) [hep-ph/9701392].
- [21] V. Barger, J.L. Hewett and R.J.N. Phillips, *Phys. Rev.* **D41** (1990) 3421.
- [22] B. Schrempp and M. Wimmer, *Prog. Part. Nucl. Phys.* **37** (1996) 1.
- [23] H.E. Haber and R. Hempfling, *Phys. Rev. Lett.* **66** (1991) 1815.
- [24] Y. Okada, M. Yamaguchi and T. Yanagida, *Prog. Theor. Phys.* **85** (1991) 1; J. Ellis, G. Ridolfi and F. Zwirner, *Phys. Lett.* **B257** (1991) 83.

- [25] S.P. Li and M. Sher, *Phys. Lett.* **B140** (1984) 339; R. Barbieri and M. Frigeni, *Phys. Lett.* **B258** (1991) 395; M. Drees and M.M. Nojiri, *Phys. Rev.* **D45** (1992) 2482; J.A. Casas, J.R. Espinosa, M. Quiros and A. Riotto, *Nucl. Phys.* **B436** (1995) 3 [E: **B439** (1995) 466].
- [26] A. Brignole, J. Ellis, G. Ridolfi and F. Zwirner, *Phys. Lett.* **B271** (1991) 123; [E: **B273** (1991) 550].
- [27] J. Ellis, G. Ridolfi and F. Zwirner, *Phys. Lett.* **B262** (1991) 477.
- [28] M. Carena, J.R. Espinosa, M. Quiros and C.E.M. Wagner, *Phys. Lett.* **B355** (1995) 209; M. Carena, M. Quiros and C.E.M. Wagner, *Nucl. Phys.* **B461** (1996) 407.
- [29] J.F. Gunion and A. Turski, *Phys. Rev.* **D39** (1989) 2701; *Phys. Rev.* **D40** (1989) 2333.
- [30] A. Brignole, *Phys. Lett.* **B277** (1992) 313.
- [31] M.A. Díaz and H.E. Haber, *Phys. Rev.* **D45** (1992) 4246.
- [32] M.S. Berger, *Phys. Rev.* **D41** (1990) 225; A. Brignole, *Phys. Lett.* **B281** (1992) 284; M.A. Díaz and H.E. Haber, *Phys. Rev.* **D46** (1992) 3086.
- [33] R. Hempfling and A.H. Hoang, *Phys. Lett.* **B331** (1994) 99.
- [34] P.H. Chankowski, S. Pokorski and J. Rosiek, *Phys. Lett.* **B274** (1992) 191; *Nucl. Phys.* **B423** (1994) 437; A. Yamada, *Phys. Lett.* **B263** (1991) 233; *Z. Phys.* **C61** (1994) 247; A. Dabelstein, *Z. Phys.* **C67** (1995) 495; D.M. Pierce, J.A. Bagger, K. Matchev and R. Zhang, *Nucl. Phys.* **B491** (1997) 3.
- [35] R. Barbieri, M. Frigeni and F. Caravaglios, *Phys. Lett.* **B258** (1991) 167; Y. Okada, M. Yamaguchi and T. Yanagida, *Phys. Lett.* **B262** (1991) 54; D.M. Pierce, A. Papadopoulos and S. Johnson, *Phys. Rev. Lett.* **68** (1992) 3678; K. Sasaki, M. Carena and C.E.M. Wagner, *Nucl. Phys.* **B381** (1992) 66; R. Hempfling, in *Phenomenological Aspects of Supersymmetry*, edited by W. Hollik, R. Rückl and J. Wess (Springer-Verlag, Berlin, 1992) p. 260–279; J. Kodaira, Y. Yasui and K. Sasaki, *Phys. Rev.* **D50** (1994) 7035.
- [36] J.R. Espinosa and M. Quiros, *Phys. Lett.* **B266** (1991) 389.
- [37] H.E. Haber and R. Hempfling, *Phys. Rev.* **D48** (1993) 4280.
- [38] H.E. Haber, R. Hempfling and A.H. Hoang, hep/ph-9609331 (1996), *Z. Phys. C* (1997), in press.

- [39] T.P. Cheng, E. Eichten and L.-F. Li, *Phys. Rev.* **D9** (1974) 2259.
- [40] N. Cabibbo, L. Maiani, G. Parisi and R. Petronzio *Nucl. Phys.* **B158** (1979) 295.
- [41] For a recent study of color and electric charge breaking minima in the MSSM and references to earlier works, see J.A. Casas, A. Lleyda and C. Muñoz, *Nucl. Phys.* **B471** (1996) 3.
- [42] H.E. Haber, R. Hempfling and Y. Nir, *Phys. Rev.* **D46** (1992) 3015.
- [43] A. Djouadi, H.E. Haber and P.M. Zerwas, *Phys. Lett.* **B375** (1996) 203; F. Boudjema and E. Chopin, *Z. Phys.* **C73** (1996) 85.
- [44] V. Barger, M.S. Berger, A.L. Stange and R.J.N. Phillips, *Phys. Rev.* **D45** (1991) 4128; J.F. Gunion, R. Bork, H.E. Haber and A. Seiden, *Phys. Rev.* **D46** (1992) 2040; J.F. Gunion, H.E. Haber and C. Kao, *Phys. Rev.* **D46** (1992) 2907; Z. Kunszt and F. Zwirner, *Nucl.Phys.* **B385** (1992) 3; A. Yamada, *Mod. Phys. Lett.* **A7** (1992) 2877.
- [45] J.F. Gunion, A. Stange and S. Willenbrock, in *Electroweak Symmetry Breaking and New Physics at the TeV Scale*, edited by T.L. Barklow, S. Dawson, H.E. Haber, and J.L. Siegrist (World Scientific, Singapore, 1996) pp. 23–145.
- [46] H.E. Haber *et al.*, hep-ph/9703391 (1997), summary report of the Weakly-Coupled Higgs Boson and Precision Electroweak Physics Working Group, to appear in the Proceedings of the 1996 Snowmass Workshop on New Directions in High Energy Physics, 25 June–12 July, 1996.
- [47] J.F. Gunion *et al.*, hep-ph/9703330 (1997), Higgs Boson Discovery and Properties Subgroup Report, to appear in the Proceedings of the 1996 Snowmass Workshop, *op. cit.*
- [48] K. Inoue, A. Kakuto and Y. Nakano, *Prog. Theor. Phys.* **63** (1980) 234; H. Komatsu, *Prog. Theor. Phys.* **67** (1982) 1177; K. Inoue, A. Kakuto, H. Komatsu and S. Takeshita, *Prog. Theor. Phys.* **67** (1982) 1889; **68** (1982) 927 [E: **70** (1983) 330] **71** (1984) 413; C. Hill, C.N. Leung and S. Rao, *Nucl. Phys.* **B262** (1985) 517; J. Bagger, S. Dimopoulos and E. Masso, *Phys. Lett.* **156B** (1985) 357; *Phys. Rev. Lett.* **55** (1985) 920.